Evaluation of Equivalent Cladding Reacted parameters of Cr-coated claddings oxidized in steam at 1200 °C in relation with oxygen diffusion/partitioning and post-quench ductility

J. C. Brachet, Matthieu Le Saux, J. Bischoff, H. Palancher, Raphaël Chosson, Édouard Pouillier, Thomas Guilbert, Stéphane Urvoy, G. Nony, Thierry Vandenberghe, et al.

Paper submitted to Journal of Nuclear Materials

Title: "Evaluation of Equivalent Cladding Reacted parameters of Cr-coated claddings oxidized in steam at 1200°C in relation with oxygen diffusion/partitioning and post-quench ductility"

Authors: J.C. Brachet[1,(*)], M. Le Saux[1,2], J. Bischoff[3], H. Palancher[4], R. Chosson[3], E. Pouillier[5], T. Guilbert[1], S. Urvoy[1], G. Nony[1], T. Vandenberghe[1], A. Lequien[1], C. Miton[1], P. Bossis[6]

Affiliations:
[1] DEN-Service de Recherches Métallurgiques Appliquées (SRMA), CEA, Université Paris-Saclay, 91191 Gif-sur-Yvette, France
[2] *Present address: ENSTA Bretagne, UMR CNRS 6027, IRDL, F-29200, Brest, France*
[3] Framatome, 10 rue Juliette Récamier, 69456 Lyon, Cedex 06, France
[4] DEN-DEC, CEA, F-13108 Saint-Paul-lez-Durance, France
[5] EDF R&D, Département MMC, avenue des Renardières, 77818 Moret-Sur-Loing, France
[6] DEN-DMN, CEA, Université Paris-Saclay, 91191 Gif-sur-Yvette, France

(*) corresponding author: jean-christophe.brachet@cea.fr

ABSTRACT:
Cr-coated M5$_{Framatome}$[1] cladding materials are studied and developed within the CEA-Framatome-EDF French nuclear fuel joint program as Enhanced Accident Tolerant Fuel claddings for Light Water Reactors. The objective of this paper is to bring some insights into the relationship between Equivalent Cladding Reacted (ECR) parameters, oxygen diffusion/partitioning and Post-Quench (PQ) ductility of Cr-coated M5$_{Framatome}$ fuel claddings oxidized in steam at 1200 °C.

The physical meaning of the ECR parameter, evaluated experimentally from the measured Weight Gain (WG) or calculated using time and temperature correlations such as the Baker-Just (BJ) or Cathcart-Pawel (CP) kinetics correlations, is discussed in the light of the benefit brought by Cr coating to oxidation resistance of cladding. As shown in this article, when applied to the Cr-coated M5$_{Framatome}$ materials, the "experimental" ECR derived from WG does not have the same physical meaning than for the uncoated cladding materials. As discussed in the paper, this is fundamentally due to the use of the ECR as a surrogate for retained ductility for uncoated claddings, and to the differences between uncoated and Cr-coated cladding in the high temperature (HT) steam oxidation processes and partitioning of the oxygen between the different layers of the oxidized cladding.

It is shown in this article that Cr-coated M5$_{Framatome}$ cladding brings significant additional time-at-temperature before full embrittlement of the cladding after one-sided oxidation at 1200 °C and quenching, compared to uncoated materials. The oxidation times and associated Baker-Just ECR (BJ-ECR) values, above which the cladding becomes brittle after low temperature quenching, are respectively ten times and three times higher than the ones for the uncoated reference cladding. When analyzing the PQ ductility of the Cr-coated M5$_{Framatome}$ cladding using a similar methodology as the one used to derive the ECR criterion for uncoated cladding, the 1-2% ductility limit corresponds to a BJ-ECR of about 50 % or higher, for a 12-15 µm-thick Cr-coated cladding tested herein.

KEYWORDS: Enhanced Accident Tolerant Fuel, Cr-coated M5$_{Framatome}$, LOCA, High Temperature Steam Oxidation, Equivalent Cladding Reacted, Post-Quenching Ductility, Oxygen Diffusion and Partitioning

[1] M5$_{Framatome}$ is a trademark or a registered trademark of Framatome or its affiliates in the USA or other countries.

HIGHLIGHTS:

- New insights are gained into the relationship between ECR parameters, oxygen diffusion/partitioning and post-quenching ductility of Cr-coated $M5_{Framatome}$ nuclear fuel claddings one-sided steam oxidized at 1200 °C
- Expressed with the Baker-just correlation, the ECR threshold leading to the post-quenching embrittlement of 12-15 µm thick Cr-coated $M5_{Framatome}$ cladding after one-sided oxidation at 1200°C is higher than 50 %, and thus at least three times higher than the historical ECR criterion of 17 % for LOCA.

1. INTRODUCTION

Among the prolific Enhanced Accident Tolerant Fuels or Advanced Technology Fuels (EATF) concepts studied worldwide, chromium-coated zirconium-based nuclear fuel claddings appeared to be a promising near term concept [1]-[12]. At CEA, prospective studies on coated zirconium claddings begun several years before the Fukushima events, as described in [13]. From these early studies, chromium-based coatings on zirconium claddings associated with a Physical Vapor Deposition (PVD) process were selected due to its significant improvement of the cladding HT steam oxidation behavior. More recent studies have been carried out on Cr-coated low-tin Zircaloy-4 and $M5_{Framatome}$ cladding materials within the CEA-Framatome-EDF French nuclear fuel joint program. These studies have shown that, the Cr-coating solution, such as the one tested herein, provides benefits in both nominal in-service conditions (negligible corrosion, increased wear resistance…) and hypothetical High Temperature (HT) accident conditions, such as Loss-Of-Coolant-Accident (LOCA) and beyond [13]-[25].

The development of these innovative fuel designs raises the question of the meaning of the historical ECR calculation using Baker-Just correlation when applied to the Cr coated cladding, especially the ones for postulated LOCA. These new solutions provide enhanced behavior in high temperature steam environment but could exhibit different degradation and failure mechanisms than the ones of the standard fuel, e.g. UO_2 fuel pellets encased in a zirconium alloy cladding [76]. This topic is notably addressed by the NEA Working Group for Fuel Safety [77].

As an EATF solution, the Cr-coated $M5_{Framatome}$ cladding improves the cladding behavior in accident conditions, and more specifically HT oxidation in LOCA. Consequently, it brings additional time at temperature and improves the post-quench ductility as shown in Figure 1 - (a). Nevertheless, if similar methodologies as for uncoated zirconium alloys and “experimental” ECR derived from the Weight Gain (WG) measurements as in Figure 1 - (b) are used, the PQ ductility may seem to be reduced. Similar results were presented by Krejci *et al.* [12] (Figure 2) and highlighted in the recent report by PNNL in “*Degradation and Failure Phenomena of Accident Tolerant Fuel Concepts Chromium Coated Zirconium Alloy Cladding*” [76]. These observations emphasize some questions regarding:

- the physical meaning of an “experimental” ECR based on WG measurements in the case of Cr-coated materials, and the use and applicability of correlations defined for uncoated zirconium cladding;he applicability of the usual “LOCA clad experimental embrittlement limit”, based on the calculated BJ-ECR parameter, to the Cr-coated materials.

The goal of this article is to clarify the HT oxidation and post-quenching embrittlement processes of the Cr-coated claddings, and to discuss how to calculate a relevant ECR for such materials. To this end, a brief review of the ECR history is presented, tracing the rationale behind this calculation, in relation with the HT oxidation-induced embrittlement of zirconium alloys. The article discusses the differences in behavior between uncoated and coated zirconium alloys in LOCA conditions based on results available from the CEA-Framatome-EDF French nuclear joint program and from Krejci *et al.* [12]. The uncoated and Cr-coated samples were oxidized and fully characterized along the following key points: oxidation kinetics, resulting microstructure (*i.e.*, *oxygen diffusion and partitioning within the wall clad thickness*) and post-quench mechanical properties. Additional experimental insights and further discussion on the specific underlying metallurgical oxidation mechanisms are presented in another paper [75]. Finally, compared to uncoated materials, this paper presents results related to the increased HT oxidation time before achieving PQ embrittlement, for the specific Cr-coated product herein.

2. HISTORICAL CONTEXT FOR THE DEFINITION OF THE ECR CRITERION

2.1. The ECR limit and parameter

For postulated LOCA events, safety criteria for Emergency Core Cooling Systems (ECCS) are defined in the US regulatory 10 CFR §50.46 [47]. Two of these criteria, the peak cladding temperature (PCT) limit of 1204 °C and the maximum cladding oxidation limit of 17 % (also called ECR limit, Equivalent Cladding Reacted – calculated using the Baker-Just correlation, see below) aim to prevent from an excessive embrittlement of fuel claddings, resulting from their HT oxidation in steam. Such an embrittlement could undermine the ability to cool the core during and after the accident transient.

The ECR parameter is defined as the fraction of zirconium consumed (in relation to the initial metallic clad thickness) with the assumption that all the oxygen having reacted with the cladding during oxidation and having diffused through the material has led to the formation of stoichiometric ZrO_2. In other words, the ECR is a simplified and macroscopic metric of the oxidation state. For the calculation of the ECR parameter, it is required in most countries to use specific oxidation kinetics correlations, identified from experimental steam oxidation tests on Zircaloy-4, such as Baker-Just (BJ) – the historical one - correlation [26] or Cathcart-Pawel (CP) correlation [27].

2.2. HT oxidation and PQ mechanical behavior of zirconium alloys

Before reminding the rationale behind the ECR criterion, one must recall the processes of the HT steam oxidation of zirconium-based claddings and of the induced embrittlement. The process shown in Figure 3 leads to the formation of a stratified material, with some more or less wavy interfaces between each major phase.

At HT in steam, zirconium alloys are oxidized and generally, in the absence of « breakaway » oxidation and/or steam starvation conditions, a dense and protective layer of zirconia forms on the metallic surface. As the oxidation reaction takes place at the oxide/metal interface, oxygen has to diffuse through the growing zirconia layer in order to reach this interface and oxidize the metal. As a result, the oxidation rate decreases with time as it is driven by this diffusion process and typical observed kinetics are nearly parabolic [26]-[31].

At these HT (> 800 °C), a fraction of the oxygen available at the oxide/metal interface is absorbed in the metal instead of reacting to form zirconia. Oxygen diffuses through the cladding thickness and the oxygen-stabilized α(O) phase appears for local oxygen concentrations superior to ~2 wt. % and up to ~7 wt. %. Depending on the temperature, the α and β phases predominate in the metallic bulk or are mixed together. The β-phase can sustain an oxygen enrichment, up to 0.5-0.6 wt. % at about 1200 °C (Figure 3).

The PQ mechanical behavior of HT oxidized claddings is usually estimated by performing Ring Compression Tests (RCT) at 20 or 135 °C. An apparent “residual ductility” is estimated from these tests, as defined as the measured displacement at failure normalized to the initial clad outer diameter. A limit of 1 or 2 % on this parameter derived from PQ RCT measurements has been proposed to define the macroscopic PQ clad Ductile-to-Brittle Transition (DBT) [30]-[55].

2.3. The origin and evolution of the ECR limit

As described in-depth in [42]-[44], the ECR limit was derived from early works performed in the sixties and the early seventies [45]-[47] with the aim of guarantying sufficient retention of ductility of the cladding after HT oxidation and quench, which was examined notably through RCT. At that early time, the main experimental programs to define the PQ ductility limit on high-tin Zircaloy-4 were performed by Hobson and Rittenhouse [55] with RCT.

At that time, it was well understood that the embrittlement of zirconium alloys is caused by the diffusion of oxygen into the metal underneath the surface oxide rather than by the surface oxide itself. In other words, the cladding residual structural integrity is controlled by the small fraction of oxygen that is dissolved in the remaining β zirconium layer, as successively later reassessed by Sawatzki [68],

Chung & Kassner [69], and more recently, for both Zircaloys and Nb-containing alloys, by Brachet et al. [57] and by Négyesi et al. [70].

Indeed:
- The zirconia and oxygen-enriched α-phase are brittle at low temperature and therefore do not contribute to the PQ cladding ductility.
- The prior-beta phase exhibits significant ductility (and mechanical resistance) at 135 °C only for oxygen content lower than a specific threshold, above which the prior-β phase is brittle at low temperature. At the time, the threshold value was estimated to be about 0.7 wt. %. Based on direct fractography examinations of PQ specimens impact tested at Room Temperature (RT), CEA studies [57] highlighted a prior-β oxygen content threshold of about 0.4 wt. %, thus making the PQ residual ductility even more sensitive to the oxygen diffusion for such PQ mechanical testing conditions.

Lacking a better method of calculating oxygen distribution in the metallic layers, the USAEC regulations used the required 17 % ECR based on BJ correlation as a surrogate measure of the time required to diffuse enough oxygen into the underlying metal to embrittle it. More generally, as resumed by Hache and Chung [42], one has to keep in mind that "the 1204 °C PCT and the 17 % ECR limits [tied with the use of BJ correlation] are inseparable, and as such, constitute an integral criterion".

Recently, additional criteria based on hydrogen contents have been proposed, but all rely on a surrogate ECR, calculated with time and temperature [48]-[51].

3. EXPERIMENTAL PROCEDURES

The studies presented here were carried out on $M5_{Framatome}$ cladding tube samples with a 12-15 µm-thick Cr-coating on their outer surface. A specific PVD-type process has been applied for chromium deposition. The typical microstructure of the as-received Cr-coated $M5_{Framatome}$ has already been presented in [13] and [22]. The Cr coatings of this product are fully dense and homogenous in thickness, with a very good bonding to the $M5_{Framatome}$ substrate. Importantly, the as-received $M5_{Framatome}$ microstructure is not affected by the coating process so that its already assessed microstructural and mechanical properties are preserved [13][17]-[19].

One-sided steam oxidation, PQ mechanical testing and metallurgical examination including micro-chemical analysis have been carried out on several CEA's facilities, described in [56]-[59]:

- For oxidation in steam up to 1250 °C, the "DEZIROX 1" facility was used since it is a reference device at CEA for HT steam oxidation. To prevent steam from coming into contact with the cladding inner surface, end caps in Zircaloy-4 were welded under secondary vacuum at both extremities of the 15 cm-long samples. For the Cr-coated cladding samples, the coating was performed on pre-welded samples to prevent any bias from differential oxidation of the end-plug and the cladding.
- PQ RCTs have been performed at both 20 °C and 135 °C on 1 cm-long clad segments. The fracture surface of the samples was examined after testing by using Scanning Electron Microscopy (SEM) to assess the PQ failure mode.
- For Nb-containing zirconium based alloys such as $M5_{Framatome}$, PQ phases/layers thickness measurements using conventional optical microscopy is more complicated than the ones for conventional Zircaloy, due to the formation and thickening of an intermediate $\alpha_{Zr}(O)$ + prior-β_{Zr} layer upon the HT oxidation process [56]. As depicted in Figure 4, image analysis procedure was developed and applied on SEM micrographs — using Back Scattered Electron (BSE) imaging mode with enhanced "phase contrast" — to measure accurately the PQ phases/layers thicknesses. Such a procedure has been already described in details in [57].
- Finally, to get more insights into the relationship between oxygen diffusion throughout the wall clad thickness and the PQ mechanical behavior, Electron Probe Micro-Analysis (EPMA) was carried out on PQ specimens. EPMA "band-scan" mode (band width of 50 µm) was preferred for smoothing the local oxygen spatial fluctuations (Figure 5). More details on the EPMA conditions applied can be found in [57].

4. ECR PARAMETER FOR UNCOATED $M5_{Framatome}$ ONE-SIDED OXIDIZED IN STEAM AT 1200 °C

Table 1 summarizes the weight gains, the thicknesses of the phases/layers and the values of the ECR parameters for reference uncoated $M5_{Framatome}$ one-sided steam oxidized at 1200 °C and directly quenched [31] [57]. The "experimental" ECR values was calculated using two methods:

(1) from the measured WG (ECR_{WG}) and taking into account the initial clad thickness (h = 0.57 mm for most cases) and outer diameter (D_o ~ 9.5 mm). This value is simply proportional to the ECR_{WG}:

Equation 1 - One-sided oxidation - $ECR_{WG} = 43.9\ [(WG/h)/(1 - h/D_o)]$ from [30]

where ECR is in %, WG is in g/cm², h and Do are in cm

Such an ECR value is representative of an overall "experimental" ECR based on the total oxygen that reacted with the tested cladding segments. For the one-sided steam oxidation experiments carried out here, the additional contribution of the oxidation of the end caps surfaces on the overall measured WG was taken into account *(it has been checked in the past that, overall, end caps oxidation kinetics was quite comparable to the one of the outer tubular clad surface)*. Additionally, it was checked that there was no significant thermal gradient induced by the HT oxidation facility used and that the oxidation was uniform both axially and circumferentially *(i.e., ~1 % max. absolute variation of the locally measured ECR value along the tested 165 mm length clad segments*).

(2) from the integration of the oxygen diffusion profiles measured by EPMA *("band-scan" mode, 50µm width*) across the metallic part of the wall cladding thickness (Figure 5-(b)) added to the contribution of the outer oxide thickness (Equation 2):

Equation 2 – ECR_{EPMA} (%) = 100 x { (X_{ZrO2} / PB) + ($[O]_{metal}$ x X_{metal} / 66.6) } / X_0

Where,

- PB is the Pilling-Bedworth coefficient [73] (about 1.56) corresponding to the ratio of the molar volume of the oxide to the molar volume of the metal. In the present case, the PB ratio corresponds to the increase in thickness associated to the formation of zirconia.

- X_0, X_{ZrO2} and X_{metal} are the respective thicknesses of the as-received clad, the outer oxide scale and the residual metallic substrate (*i.e., $\alpha_{Zr}(O)$ + prior-β_{Zr} layers)*.

- $[O]_{metal}$ is the average atomic concentration of oxygen within the remaining metallic substrate derived from oxygen diffusion profiles measured by EPMA (Figure 5-(b)); it has been checked that oxygen diffusion was homogenous circumferentially and thus that the measured oxygen profile (in "Band-scan" mode) was statistically representative.

This last approach would be especially interesting when weighing is not possible and/or when the tested claddings have been subjected to heterogeneous HT oxidation, as experienced upon LOCA integral tests for example.

Table 1 – Weight gains, phases/layers thicknesses and ECR parameters values for reference uncoated $M5_{Framatome}$ one-sided steam oxidized at 1200 °C and directly quenched:

Oxidation time at 1200 °C (s)	WG (mg/cm²)	ZrO_2 (µm)	$\alpha_{Zr}(O)$ (µm)	$\alpha_{Zr}(O)$ + prior-β_{Zr} (µm)	Prior-β_{Zr} (µm)	"Exp." ECR from WG (%)	"Exp." ECR from EPMA (%)	BJ-ECR (%)
60	4.7	19	19	26	555	3.4	2.6	5.0
200	8.7	45	51	34	497	7.0	6.3	9.2
560	15-16	73	82	61	416	12.1	11.1	15.4
1420	22.5 - 24.5	122	148	142	207	18.5	19.2	25.9
3075	35-36	n. m.	n. m.	n. m.	n. m.	28.6	n. m.	38.1
6000	~49	n. m.	n. m.	n. m.	n. m.	39.4	n. m.	53.3

n. m. stands for not measured

Figure 6 compares the ECR values determined from experimental measurements and the values calculated by using the BJ and CP parabolic correlations, as a function of the oxidation time at 1200 °C. This plot confirms the parabolic kinetics of steam oxidation of $M5_{Framatome}$ at 1200 °C. A very good agreement between the two "experimental" evaluations of ECR is observed. This is likely due to a good accuracy of EPMA oxygen diffusion profiles measurements together with a good uniformity of the HT oxidation. Finally, it is confirmed that the BJ-ECR values are quite conservative and thus are higher than the CP-ECR, these last ones being very close to the experimental ones.

Figure 7 depicts the oxygen through-thickness profile measured by EPMA and associated SEM micrographs for reference uncoated $M5_{Framatome}$ oxidized for 1500 s at 1200°C. For this oxidation condition, nearly half of the initial clad wall thickness has been transformed into ZrO_2 and $\alpha_{Zr}(O)$ layers (brittle at low temperature) and the oxygen concentration within the residual inner prior-β_{Zr} layer reaches ~0.6 wt. %. This last oxygen concentration value is very close to the equilibrium oxygen solubility in β_{Zr} calculated for Zr-1%Nb alloy at 1200 °C using the Thermo-Calc® software associated with the thermodynamic database for zirconium alloys developed at CEA [71][72]. This means that after one-sided steam oxidation at 1200 °C for 1500 s (and beyond) the oxygen content in the residual inner prior-β_{Zr} layer is higher than the critical value (*i.e.*, ~0.4 wt. %) inducing a DBT for prior-β_{Zr} at RT [57]. This explains why the PQ macroscopic behavior of this particular sample is nearly brittle, as highlighted by the fractographs and the low residual ductility values measured after PQ RCTs which will be further compared with the Cr-coated material ones.

5. OXIDATION OF CR-COATED $M5_{Framatome}$ IN STEAM AT 1200 °C

The evolution of weight gain as a function of one-sided steam oxidation time at 1200 °C is plotted in Figure 8 for both uncoated and 12-15 µm Cr-coated $M5_{Framatome}$. Due to the protective effect of the outer Cr-coating, the coated $M5_{Framatome}$ cladding shows a significant reduction in the HT oxidation by comparison to the uncoated material. Photographs of some of the tested clad segments are also given in Figure 8. It appears that there is a critical oxidation time at 1200 °C above which the tested samples break into pieces upon the final direct water quenching (here, without application of any additional axial loading). This critical time ranges between 3000 s and 6000 s (38 % < BJ-ECR < 53 %) for uncoated reference $M5_{Framatome}$ and between 9000 s and 12000 s (65 % < BJ-ECR < 75 %) for Cr-coated $M5_{Framatome}$. This observation confirms the additional time until the structural failure upon quench. In other words, the capacity of the cladding oxidized at HT to withstand the final quenching for the same time-at-temperature is significantly improved by the outer Cr coating.

Additionally, Optical Micrographs (OM) of post-oxidized/quenched Cr-coated samples are shown in Figure 8. At this scale, one can observe various microstructural evolutions of the metallic substrate as a function of the one-sided oxidation time at 1200 °C:

- For times < 5000-6000 s, the weight gain is low and the Cr-coating is protective as no zirconia or $\alpha_{Zr}(O)$ incursions are observed within the (full) prior-β_{Zr} metallic substrate beneath the residual outer Cr scale. As a reminder, for the uncoated reference material, within the same oxidation time range, up to about two-thirds of the initial metallic clad thickness is transformed into brittle zirconia and $\alpha_{Zr}(O)$ layers.
- For times > 5000-6000 s, an acceleration of the weight gain is observed, which is associated with a loss of protectiveness of the Cr-coating linked with the formation of a ZrO_2 layer under the remaining Cr-coating and the growth of a thick $\alpha_{Zr}(O)$ layer.

Between these two major oxidation stages, the transition observed at about 5000-6000 s is characterized by the partial loss of protectiveness of the Cr-coating allowing oxygen diffusion in the substrate without formation of a zirconia layer. The oxidation-induced microstructural and micro-chemical evolutions of Cr-coated $M5_{Framatome}$ for each of these two stages will be analyzed in more detail hereafter before assessing the relation with its PQ ductility derived from RCT. A deep discussion of the underlying oxidation mechanisms of the Cr-coating itself is outside the scope of the present paper and is then fully described in another dedicated paper [75]. However, to summarize the specific HT oxidation process of Cr-coated zirconium based claddings, it must be noticed first that, consistently with previously published HT oxidation kinetics data for bulk chromium, the overall oxidation kinetics is nearly parabolic at the beginning of oxidation, when the Cr outer layer is protective. Finally, it significantly accelerates, and hydrogen is absorbed during a short intermediate period. These steps correspond to different underlying oxidation and diffusion mechanisms, involving:

- Formation and growth of outer chromia scale simultaneously with chromium diffusion into the β_{Zr} zirconium substrate,

- Zr-Cr interdiffusion, inducing $Zr(Cr,Fe)_2$ intermetallic layer thickening, and then disappearance at longer oxidation times due to re-transformation to metallic chromium and to zirconia (*i.e., when the Cr-coating is no more protective, inducing a high inward flux of oxygen into the β_{Zr} zirconium substrate*),

- Transport of oxygen through the residual metallic chromium layer (*in particular along grain boundaries with formation of a continuous zirconia network*) and then into the zirconium substrate,

- And finally, when the residual sub-oxide metallic layer has been mainly consumed (*by both outer chromia scale formation and chromium diffusion into the zirconium substrate*) and due to residual coating multi-cracking occurrence, growth of sub-coating zirconia. This last situation occurs when the inward flux of oxygen into the β_{Zr} zirconium substrate is high enough.

Microstructural analysis of Cr-coated cladding oxidized at 1200 °C for 1500 s (times < 5000-6000 s):

Preliminary remark: thanks to its quite low thermal diffusivity and its thermodynamic affinity to the β_{Zr} phase, niobium displays a specific partitioning behavior upon HT oxidation process, inducing some microstructural and micro-chemical fluctuations within the post-oxidized zirconium structure [56]. However, in the following, we will focus only on chromium and oxygen behavior upon the HT oxidation process because diffusion and partitioning of these chemical species are believed to be mainly responsible for the PQ coated clad mechanical properties evolution. While, based on previous results obtained on uncoated $M5_{Framatome}$ [57], niobium partitioning occulting upon HT oxidation seems to have limited effect (if any) on the PQ clad properties.

The optical micrographs in Figure 9 show a few micrometers-thick outer chromia scale with a ~10 µm-thick sub-oxide residual chromium (non-oxidized) metallic layer. These observations confirm that for these oxidation conditions, the Cr-coating has prevented the under-coating prior-β_{Zr} metallic substrate from oxygen ingress. Figure 9 gives more detailed informations on chemical species diffusion and partitioning. Consistent with the very low WG measured, EPMA measurements show no significant oxygen diffusion within the prior-β_{Zr} metallic substrate. A slight oxygen uptake via the inner clad surface can be noticed. It is likely due to some residual air trapped into the inner clad volume (*the closed inner clad volume is under secondary vacuum, but for some samples, a small residual oxygen partial pressure may be present*). Additionally and as already discussed in [13], EPMA measurements highlight some chromium diffusion that has occurred within the prior-β_{Zr} metallic substrate; such phenomena may induce some localized prior-β_{Zr} hardening but a deep discussion on this additional metallurgical effect is outside the scope of the present paper.

Microstructural analysis of Cr-coated cladding oxidized at 1200 °C for 9000 s (times > 5000-6000 s):

For such extreme oxidation times, uncoated $M5_{Framatome}$ is heavily oxidized (BJ-ECR ~ 65 %) and would not survive water quenching while the 12-15 µm Cr coated $M5_{Framatome}$ segment did. For these severe oxidation conditions, the coated materials show a nearly brittle PQ macroscopic behavior during PQ RCT carried out at RT.

It must be mentioned that even if PQ residual ductility of HT oxidized cladding is low, this does not necessarily mean that the sample does not survive to the water quenching. This is for example the case for uncoated zirconium alloys after steam oxidation for 1500 s at 1200 °C showing low residual ductility at RT while surviving to the final water quenching.

Concerning Cr-coated materials in Figure 8 and Figure 10, for long oxidation times such as 9000 s, the outer Cr coating is no more protective and leads to a brittle behavior since most of the residual Zr-based metallic substrate has been converted to brittle $\alpha_{Zr}(O)$ [76]. It is important to highlight that at the same time, only a few tens of micrometers of the outer clad thickness has been transformed into (Cr_2O_3 + ZrO_2) oxide scales. This last observation shows that, after HT oxidation, the ratio between the thicknesses of $\alpha_{Zr}(O)$ and outer oxide scales is very different for Cr-coated and uncoated materials. In other words, upon HT oxidation, the Cr coating significantly slows down the formation (and subsequent thickening) of under-coating zirconia layer than on the growth of $\alpha_{Zr}(O)$, while for conventional uncoated claddings, zirconia and $\alpha_{Zr}(O)$ have comparable growth kinetics, as it can be observed in Table 1.

Additionally, in Figure 10, it can be observed that there are significant fluctuations of the Cr concentration along the chromium diffusion profile. In fact, even if it has not been plotted here for sake of simplicity, these fluctuations are correlated to the niobium partitioning/fluctuations already mentioned. Indeed, as for niobium [56], chromium has a higher thermodynamic affinity to the β_{Zr} phase and thus tends to segregate into some residual thin prior-β_{Zr} zones upon the $\alpha_{Zr}(O)$ growth thickening process for this high oxidation time.

6. ANALYSIS OF THE DIFFUSION OF OXYGEN IN THE ZIRCONIUM SUBSTRATE FOR CR-COATED CLADDING OXIDIZED IN STEAM AT 1200 °C

Table 2 summarizes the weight gains (WG), the phases/layers thicknesses and the ECR parameters of 12-15 µm Cr-coated $M5_{Framatome}$ cladding samples after one-sided steam oxidation at 1200 °C followed by direct water quenching down to RT. This Table shows a significant difference for the Cr-coated cladding between the ECR_{WG} and the BJ-ECR, unlike the results shown in section 3 on uncoated cladding. So unlike for uncoated cladding, ECRWG and ECR BJ cannot be used indiscriminately as they differ by order of magnitude in the case of Cr coated claddings. Both ECRs cannot be confused and one must keep in mind which is which.

Table 2 - Weight gains, phase/layer thicknesses and ECR parameters of 12-15 µm Cr-coated $M5_{Framatome}$ after one-sided steam oxidation at 1200 °C and direct quenching:

Oxidation time at 1200 °C (s)	WG (mg/cm²)	ZrO_2 thickness (µm)	$\alpha_{Zr}(O)$ thickness (µm)	$\alpha_{Zr}(O)$+ prior-β_{Zr} thickness (µm)	Prior-β_{Zr} thickness (µm)	ECR_{WG} (*) (%)	BJ-ECR (*) (%)
600	~1.2	0	0	0	575	0.9	16.8
1500	1.5	0	0	0	575	1.2	26.6
3000	2.5	0	0	0	575	2.0	37.7
5000	4.7	n. r.(**)	n. r.(**)	n. r.(**)	n. r.(**)	3.8	48.6
6000	>6 - 7.4	~0	~25	~500 - 550	~0 - 50	~5 - 6	53.3
9000	15.6 - 18.7	~10 - 30	~200 - 250	~300 - 350	0	12.5 - 15	65.2
12000	32.4	45 - 65	~400	<50	0	26.1	75.3

(*) calculated for 0.57 mm-thick uncoated cladding
(**) not relevant, because of significant inner oxidation contribution (due to residual oxygen trapped inside this particular end-plugged clad segment); thus, should be more or less considered as a two-sided oxidized sample…

This table shows that this 12-15 µm-thick Cr-coating is fully protective for oxidation times up to at least 3000 s at 1200 °C, corresponding to an approximate BJ-ECR of at least 40 %. For longer oxidation times, the coating allows a progressive in-coming oxygen diffusion within the underlying metallic substrate, which leads first to a thickening of a $\alpha_{Zr}(O)$ layer and then, at longer oxidation times, to the formation of a zirconia layer under the coating [75].

Additionally, results given in Table 3 were derived from oxygen profiles measured by EPMA and the measured outer oxide scale thicknesses. These results further justify the difference in behavior between uncoated and Cr-coated cladding. The values reported in this Table demonstrate that the partition of oxygen between the outer oxide scales and the sub-oxide metallic substrate is very different for uncoated and Cr-coated $M5_{Framatome}$. Indeed, for the uncoated reference material, only 20 to 30 % of the overall oxygen which reacted with the clad during its oxidation at 1200°C diffused into the sub-oxide metallic substrate, whereas this value is over 85 % for Cr-coated cladding.

It is the prior β_{Zr} layer which is responsible for the retention of post quench ductility. As recalled in Figure 5-(a), at RT, the PQ DBT failure mode of prior-β_{Zr} takes place for an oxygen content of ~0.4 wt. %. It means that, beyond some potential and limited additional PQ hardening effect due to the HT chromium diffusion *(which concerns mainly the outer part of the wall clad thickness and which will be discussed elsewhere*), the "physical-metallurgical" parameter responsible for the PQ macroscopic DBT as derived from PQ RCT is directly related to the quantity of oxygen which diffused into the sub-oxide metallic substrate, rather than to the overall quantity of oxygen that reacted.

After 1500 s at 1200 °C, no significant oxygen diffusion into the β_{Zr} layer is observed in the case of the coated material. For longer oxidation times, a major part (approximately 85 % after oxidation for 9000 s) of the oxygen that reacted with Cr-coated $M5_{Framatome}$ diffused into the metallic substrate, inducing extended growth of $\alpha_{Zr}(O)$. Because most of the oxygen that reacted with the Cr-coated clad during HT oxidation diffused into the sub-oxide metallic substrate for the longer oxidation times applied here (9000-12000 s), the DBT occurs for a lower measured weight gain for the Cr-coated $M5_{Framatome}$. Basically, as shown in Table 3, this is due to the fact that the weight gain associated to oxygen diffusion within the prior-β_{Zr} layer (and to the growth of $\alpha_{Zr}(O)$) is at least one order of magnitude lower than the one corresponding to the growth of outer stoichiometric zirconia.

These results clearly show that the weight gain and therefore the "experimental" ECR_{WG} are not relevant indicators of the PQ material brittleness when the partition of oxygen between the outer oxides (ZrO_2 and/or Cr_2O_3) and the metallic substrate does not follow the typical partition observed in uncoated zirconium-based cladding steam oxidized at HT. It can be mentioned that such a discrepancy also exists for conventional uncoated claddings when the partition of oxygen deviates from the "usual" one, in case of "steam starvation" or "post-breakaway oxidation" for example.

Table 3 - Fraction of the "experimental" ECR_{WG} corresponding to the overall fraction of reacted oxygen which has diffused into the metallic substrate beneath the outer coating / oxide scales during oxidation at 1200 °C

Materials	**Oxidation time at 1200 °C (s)**	**WG (mg/cm²)**	**ECR_{WG} (%)**	**Fraction of ECR** corresponding to oxygen which has diffused into the metallic substrate
Uncoated $M5_{Framatome}$	60 - 1420s	4.3 - 23.5 (+/1)	3.5 - 19 (+/-1)	**20-30 %**
12-15µm Cr-coated $M5_{Framatome}$	1500	1.5	1.2	Negligible oxygen diffusion in prior-β_{Zr}
	9000	15.6	12.5	**85 %**

Finally, as an attempt to summarize the above observations, Figure 11 gives an overview of the oxygen diffusion and partitioning within the wall clad thickness of 12-15 µm Cr-coated $M5_{Framatome}$ upon one-sided steam oxidation at 1200 °C.

7. ANALYSIS OF THE CR-COATED CLADDING PQ DUCTILITY AND ITS RELATIONSHIP WITH THE BJ-ECR CRITERION

Figure 12 shows the PQ "residual ductility" obtained from RCT performed at 20 and 135 °C on uncoated and 12-15 µm Cr-coated $M5_{Framatome}$ as a function of one-sided steam oxidation time at 1200 °C and ECR parameters (calculated by using the BJ correlation (BJ-ECR) and deduced from the measured WG (ECR_{WG})). One has to keep in mind that these ECR parameters were evaluated using the conventional correlations and assumptions for uncoated claddings. As described in Section 6 and discussed in more details in [75], the diffusion of oxygen within the underlying zirconium substrate change with coated cladding. Thus, the "physical meaning" of the "experimental" ECR_{WG} is not applicable for the coated material.

The different plots in Figure 12 show that:

- on the one hand and as already observed for the resistance to quenching, when compared to reference uncoated $M5_{Framatome}$, the 12-15 µm Cr-coating exhibits a significant additional time to the PQ embrittlement threshold (Figure 12-(a)). This is also shown by the plot of the RCT ductility as a function of the calculated BJ-ECR, which is not surprising since this parameter is simply proportional to the square root of the oxidation time.
- on the other hand, the plot of RCT ductility as a function of the "experimental" ECR_{WG} (*which, as already discussed, has not the same physical meaning for coated claddings than for uncoated ones*) displays an opposite tendency. Indeed, the ECR_{WG} value corresponding to the PQ embrittlement threshold is ranging between 5 and 15 % for the Cr-coated $M5_{Framatome}$, which is significantly lower than the characteristic value for the uncoated reference $M5_{Framatome}$. The various plots in Figure 12 qualitatively confirm Krejci *et al.'* [12] data tendency (Figure 2); but the conclusion drawn from them is different since they suggest that the "ECR_{WG}" is not the appropriate parameter for Cr-coated cladding, because the ECR_{WG} does not have the same physical meaning for the Cr-coated cladding.

When further analyzing these plots (excluding the ones based on ECR_{WG}), the general aspect of the Cr-coated curves in Figure 12 a) and b) is quite different than that of the uncoated cladding with some form of plateau up to at least 3000 s, and then a clear, accelerated decrease after 5000 s. The uncoated cladding exhibits a decrease in ductility from the beginning of oxidation. In the "plateau" region for the Cr-coated cladding, there is nonetheless a slight decrease in ductility, which can likely be attributed to the diffusion of Cr in the zirconium substrate inducing some PQ prior-β_{Zr} hardening. However, the data presented here demonstrates that the Cr diffusion in the zirconium matrix has a secondary effect on the loss of ductility of the Cr-coated cladding compared to the diffusion of oxygen once the coating becomes non-protective.

These curves can help adapt the BJ-ECR criterion for application to the Cr-coated cladding using the same methodology that was used to define the initial BJ-ECR criterion of 17 %. By considering that the cladding's residual ductility limit is of 1-2 %, one can extrapolate this limit for the Cr-coated cladding, which leads to a BJ-ECR criterion around 50 % or higher for one-sided oxidation, as shown by the dotted lines in Figure 12. This shows how the BJ-ECR can be maintained to evaluate cladding embrittlement due to oxidation during a LOCA even for Cr coated cladding. Comparing the BJ-ECR for both alloys the better oxidation resistance of Cr Coated alloy is clearly evidenced.

Finally, Figure 13 depicts the PQ "residual ductility" derived from RCT carried out at both 20 and 135 °C on uncoated and Cr-coated claddings as a function of the mean oxygen content of the residual prior-β_{Zr} layer. In this figure, some previous results obtained both at UJP Praha (*Krejci et al. [12]*) and at CEA on different Cr-coated substrates, and using different coating processes, were added to extend the database. It has to be mentioned that the experimental testing and analysis procedures used at CEA (*present study*) and at UJP Praha (*Krejci et al. [12]*) sometimes differ, and thus may contribute to some bias on the results when plotted in the figure. However, the plot indicates that, as for the reference uncoated claddings, the PQ embrittlement threshold of Cr-coated claddings relies mainly on the oxygen content of the residual prior-beta layer. Thus, the observed improvement of the PQ properties of Cr-coated claddings is directly related to the capacity of the Cr-coating to delay the

inward diffusion of oxygen into the sub-coating Zr metallic substrate upon HT steam oxidation, typical of LOCA situations.

8. CONCLUSION

The objective of the present paper was to bring some insights into the relationship between "experimental" and "calculated" ECR parameters, oxygen diffusion for Cr-coated claddings oxidized in high temperature steam and how they relate to post-quench ductility. It is confirmed that, for Cr-coated $M5_{Framatome}$, the coating brings significant additional time before full clad embrittlement, following oxidation at 1200 °C and final direct water quenching down to RT. Overall, the observed improvement of the PQ properties is related to the capacity of the coating to delay the inward diffusion of oxygen into the sub-coating Zr metallic substrate upon HT steam oxidation.

<u>One-sided oxidation behavior of the Cr-coated $M5_{Framatome}$ cladding</u>

The results presented show that the one-sided steam oxidation process at 1200 °C of 12-15 µm Cr-coated $M5_{Framatome}$ includes two main steps:

1. For oxidation times < 5000 s, a dense and protective thin outer chromia scale grows without significant oxygen diffusion into the substrate. Indeed, the oxygen content of the inner prior-β_{Zr} layer is close to the as-received (nominal) value. In this case, and as it will be discussed elsewhere, the PQ clad ductility is slightly affected by the hardening and embrittlement effects of Cr having diffused into the outer part of the prior-β_{Zr} layer, but this effect is secondary to that of oxygen diffusion.

2. For longer oxidation times (> 5000 s), when the in-coming oxygen diffusion flux beneath the coating is high enough, ZrO_2 starts growing (*i.e.*, when the $C_{\alpha/ox}$ equilibrium solubility in the metallic $\alpha_{Zr}(O)$ is reached at the metal/oxide interface). At this stage, most of the underlying metallic substrate is transformed into $\alpha_{Zr}(O)$, thus inducing a macroscopic PQ brittle behavior of the cladding at RT.

In-between these two oxidation stages, there is a transition where the residual (mostly oxidized) outer chromium coating loses progressively its protective properties. In this case and as discussed in depth in [75], oxygen progressively diffuses within the metallic substrate, which leads to the growth of an under-coating $\alpha_{Zr}(O)$ layer, but without formation of ZrO_2 at this stage.

<u>Discussion on the use of the "experimental" ECR derived from WG using the uncoated cladding correlations</u>

The US LOCA ECR criterion is used together with the conservative BJ or "best-estimate" CP correlations. The BJ correlation was derived from results of oxidation tests performed on uncoated zirconium alloys.

The coated cladding shows different oxidation mechanisms, kinetics and distribution of oxygen, most of which is not used to form ZrO_2 like for the uncoated cladding. As a result, the usual interpretation of ECR_{WG}, as used for uncoated claddings, is no longer valid for Cr-coated claddings because the oxygen reacting upon HT oxidation is fully used to form an outer chromia scale for smaller oxidation times or mainly diffuses in the metallic bulk for the longer oxidation times. Therefore, the uncoated ECR_{WG} calculations should not be used to compare uncoated and coated materials since the uncoated cladding correlation is not valid for the Cr-coated cladding.

<u>Embrittlement threshold for the Cr-coated $M5_{Framatome}$ cladding and corresponding ECR limit</u>

By definition, the BJ-ECR and CP-ECR parameters are proportional to the square root of the HT oxidation time. Thus, plotting the residual PQ RCT ductility as a function of the BJ-ECR or CP-ECR (Figure 12-(b)) confirms the additional time-at-temperature observed for Cr-coated cladding when plotting the results as a function of the one-sided oxidation time. The data presented in this article

show that the oxidation time at 1200 °C leading to cladding embrittlement and the associated BJ-ECR threshold are much larger for the Cr-coated material than for the uncoated reference cladding.

Using the same methodology as that used historically to derive the ECR criterion for uncoated cladding, a 1-2 % ductility limit would correspond to about 50-% BJ-ECR for the 12-15 µm thick Cr-coated $M5_{Framatome}$ cladding one-sided oxidized in steam at 1200 °C. The current US regulatory ECR limit of 17 % calculated with the BJ correlation, is therefore highly conservative for the one-sided oxidation of the Cr-coated $M5_{Framatome}$ cladding.

Although the BJ-correlation does not accurately describe the oxidation behavior of the Cr-coated materials, it can still be used as an oxidation time-at-temperature metric. It would therefore be possible to define new BJ-ECR limits corresponding to the performance of the Cr-coated cladding using the BJ-correlation.

Alternatively, one could also establish new oxidation kinetics correlations specific to the coated materials, using the weight gain for instance, and use these correlations to define new limits preventing the cladding embrittlement in LOCA conditions. Such new correlations may vary according to the Cr-coated material used so a new standardized approach would have to be created.

In both cases, the new limits should:

- Be performance-based and thus specific to each Cr-coated cladding solution. Indeed, the protection given by the Cr-coating during high temperature oxidation depends certainly on numerous parameters, notably the coating thickness and the deposition process [13].
- Take into account the relevant phenomena occurring during LOCA transients, especially ballooning, burst and inner oxidation.

AKNOWLEDGEMENTS

Special thanks to:

- M. Le Flem and I. Idarraga (now at EDF-DT) from CEA for their initial input on the R&D on coated Zr-based alloys;

- F. Lomello, A. Michau and F. Schuster from CEA, G. Velisa and Prof. A. Billard from UTBM (Montbéliard, France), E. Monsifrot and J. Runser from DEPHIS society (Etupes, France), for PVD Cr-coated materials fabrication;

- D. Hamon from CEA, for EPMA measurements;

- T. Forgeron, J. Henry, L. Vincent, L. Portier and A. Soniak from CEA, for their advising and organizing support;

This study has been conducted under the French Nuclear R&D program between CEA, Framatome and EDF. Specific thanks to Nermine Chaari and Christine Delafoy from Framatome and, Antoine Ambard and Frédérique Rossillon from EDF.

The presented data with Cr-coated E110 alloy were produced at UJP Praha a.s. within the IAEA ACTOF project.

REFERENCES

[1] C. Tang, M. Stueber, H.J. Seifert, M. Steinbrueck, “Protective coatings on zirconium-based alloys as accident tolerant fuel (ATF) claddings”, Corros. Rev. 35 (2017) 141–165

[2] Y.-H. Koo, J.-H. Yang, J.-Y. Park, K.-S. Kim, H.-G. Kim, D.-J. Kim, et al., “KAERI’s development of LWR accident tolerant fuel”, Nucl. Technol. 186 (2014) 295–30

[3] H.-G. Kim, I.-H. Kim, Y.-I. Jung, D.-J. Park, J.-Y. Park, Y.-H. Koo, “Adhesion property and high-temperature oxidation behavior of Cr-coated Zircaloy-4 cladding tube prepared by 3D laser coating”, J. Nucl. Mater. 465 (2015) 531–539

[4] A.S. Kuprin, V.A. Belous, V.N. Voyevodin, V.V. Bryk, R.L. Vasilenko, V.D. Ovcharenko, et al., “Vacuum-arc chromium-based coatings for protection of zirconium alloys from the high-temperature oxidation in air”, J. Nucl. Mater. 465 (2015) 400–406

[5] J.H. Park, H.-G. Kim, J. Park, Y.-I. Jung, D.-J. Park, Y.-H. Koo, “High temperature steam-oxidation behavior of arc ion plated Cr coatings for accident tolerant fuel claddings”, Surf. Coatings Technol. 280 (2015) 256–259

[6] D.J. Park, H.G. Kim, Y. Il Jung, J.H. Park, J.H. Yang, Y.H. Koo, “Behavior of an improved Zr fuel cladding with oxidation resistant coating under loss-of-coolant accident conditions”, J. Nucl. Mater. 482 (2016) 75–82

[7] H. Shah, J. Romero, P. Xu, B. Maier, G. Johnson, J. Walters, et al., “Development of Surface Coatings for Enhanced Accident Tolerant Fuel”, in: Water React. Fuel Perform. Meet., Jeju Island, Korea, (2017)

[8] H.-G. Kim, I.-H. Kim, Y.-I. Jung, D.-J. Park, J.-H. Park, J.-H. Yang, et al., “Progress of Surface Modified Zr Cladding Development for ATF at KAERI”, Proceedings of Water React. Fuel Perform. Meet., Jeju Island, Korea, (2017)

[9] W. Zhong, P.A. Mouche, B.J. Heuser, “Response of Cr and Cr-Al coatings on Zircaloy-2 to high temperature steam”, Journal of Nuclear Materials 498 (2018) 137-148

[10] M. Sevecek, A. Gurgen, A. Seshadri, Y. Che, M. Wagih, B. Phillips, V. Champagne, K. Shirvan, “Development of Cr cold spray-coated fuel cladding with enhanced accident tolerance”, Nuclear Engineering and Technology (2018),

[11] Y. Wang, W. Zhou, Q. Wen, X. Ruan, F. Luo, G. Bai, Y. Qing, D. Zhu, Z. Huang, Y. Zhang, T. Liu, R. Li, “Behavior of plasma sprayed Cr coatings and FeCrAl coatings on Zr fuel cladding under loss-of-coolant accident conditions”, Surface & Coatings Technology 344 (2018) 141–148

[12] J. Krejci, M. Sevecek, J. Kabatova, F. Manoch, J. Koci, L. Cvrcek, J. Malek, S. Krum, P. Sutta, P. Bublikova, P. Halodova, H. K. Namburi, “Experimental Behavior of Chromium-Based coatings”, Proceedings of Topfuel 2018, Praha, Czech Republic (2018)

[13] J.C. Brachet, I. Idarraga-Trujillo, M. Le Flem, M. Le Saux, V. Vandenberghe, S. Urvoy, E. Rouesne, T. Guilbert, C. Toffolon-Masclet, M. Tupin, C. Phalippou, F. Lomello, F. Schuster, A. Billard, G. Velisa, C. Ducros, F. Sanchette, “Early studies on Cr-Coated Zircaloy-4 as Enhanced Accident Tolerant Nuclear Fuel Claddings for Light Water Reactors”, Journal of Nuclear Materials 517 (2019) 268-285

[14] J.C. Brachet, C. Lorrette, A. Michaux, C. Sauder, I. Idarraga-Trujillo, M. Le Saux, M. Le Flem, F. Schuster, A. Billard, E. Monsifrot, E. Torres, F. Rebillat, J. Bischoff, A. Ambard, “CEA studies on advanced nuclear fuel claddings for enhanced accident tolerant LWRs fuel (LOCA and beyond LOCA conditions)”, Proceedings of Fontevraud 8: Conference on Contribution of Materials Investigations and Operating Experience to LWRs' Safety, Performance and Reliability; Avignon (France), (15-18 Sep 2014)

[15] J. Bischoff, K. McCoy, J. Strumpell, J-C. Brachet, C. Lorrette, "Development of Fuels with Enhanced Accident Tolerance", Proceedings of TopFuel Conference 2015, Zurich, Switzerland, (Sept. 2015)

[16] J.C. Brachet, M. Le Saux, M. Le Flem, S. Urvoy, E. Rouesne, T.Guilbert, C. Cobac, F. Lahogue, J. Rousselot, M. Tupin, P. Billaud, C. Hossepied, F. Schuster, F. Lomello, A. Billard, G. Velisa, E. Monsifrot, J. Bischoff, A. Ambard, "On-going Studies at CEA on Chromium Coated

Zirconium Based Nuclear Fuel Claddings for Enhanced Accident Tolerant LWR Fuel", Proceedings of TopFuel Conference 2015, Zurich, Switzerland, (September 2015)

[17] J. Bischoff, C. Delafoy, P. Barberis, D. Perche, B. Buerin, J-C Brachet, "Development of Cr-coated Zirconium Cladding for Enhanced Accident Tolerance", Proceedings of TopFuel Conference 2016, Boise, ID, USA, (September 2016)

[18] J. Bischoff, C. Delafoy, C. Vauglin, P. Barberis, C. Roubeyrie, D. Perche, D. Duthoo, F. Schuster, J-C. Brachet, E.W. Schweitzer, K. Nimishakavi, "AREVA NP's Enhanced Accident Tolerant Fuel Developments: Focus on Cr-coated M5 Cladding", Nuclear Engineering and Technology 50 (2018) 223-228

[19] J. Bischoff, C. Delafoy, N. Chaari, C. Vauglin, K. Buchanan, P. Barberis, F. Schuster, J-C Brachet, K. Nimishakavi, "Cr-coated cladding development at Framatome", Proceedings of WRFPM/TOPFUEL 2018, (30 Sept. – 04 Oct. 2018), Prague, Czech Republic

[20] I. Idarraga-trujillo, M. Le Flem, J-C Brachet, M. Le Saux, D. Hamon, S. Muller, V. Vandenberghe, M. Tupin, E. Papin, A. Billard, E. Monsifrot, F. Schuster, "Assessment at CEA of Coated Nuclear Fuel Cladding for LWRs with Increased Margins in LOCA and beyond LOCA Conditions", Proceedings of 2013 LWR Fuel Performance Meeting/TopFuel, Charlotte, NC, USA, Sept. 15-19, (2013)

[21] J.C. Brachet, M. Le Saux, V. Lezaud-Chaillioux, M. Dumerval, Q. Houmaire, F. Lomello, F. Schuster, E. Monsifrot, J. Bischoff, E. Pouillier, "Behavior under LOCA Conditions of Enhanced Accident Tolerant Chromium Coated Zircaloy-4 Claddings", Proceedings of TopFuel 2016 Conference, Boise, ID, USA, (September 2016)

[22] J.C. Brachet, M. Dumerval, V. Lezaud-Chaillioux, M. Le Saux, E. Rouesne, D. Hamon, S. Urvoy, T. Guilbert, Q. Houmaire, C. Cobac, G. Nony, J. Rousselot, F. Lomello, F. Schuster, H. Palancher, J. Bischoff, E. Pouillier, "Behavior of Chromium Coated M5 Claddings under LOCA Conditions" Proceedings of WRFPM Conference, Jeju, Republic of South Korea, (September 2017)

[23] C. Delafoy, J. Bischoff, J. Larocque, P. Attal, L. Gerken, K. Nimishakavi, "Benefits of Framatome's E-ATF evolutionary solution: Cr-coated cladding with Cr_2O_3-doped UO_2 fuel", Proceedings of TopFuel 2018, Prague, Czech Republic, September 2018

[24] J.C. Brachet, T. Guilbert, M. Le Saux, J. Rousselot, G. Nony, C. Toffolon-Masclet, A. Michau, F. Schuster, H. Palancher, J. Bischoff, J. Augereau, E. Pouillier, "Behavior of Cr-coated M5 claddings during and after high temperature steam oxidation from 800°C up to 1500°C (LOss-of-Coolant Accident & Design Extension Conditions)", Proceedings of WRFPM/TOPFUEL 2018, (30 Sept. – 04 Oct. 2018), Prague, Czech Republic

[25] M. Dumerval, Q. Houmaire, J.C. Brachet, H. Palancher J. Bischoff, E. Pouillier, « Behavior of Chromium Coated M5 Claddings upon thermal ramp tests under internal pressure (LOss-of-Coolant Accident Conditions)", Proceedings of WRFPM/TOPFUEL 2018, (30 Sept. – 04 Oct. 2018), Prague, Czech Republic

[26] L. Baker and L.C. Just, "Studies of metal-water reactions at high temperatures. III. Experimental and theoretical studies of the zirconium-water reaction", ANL-6548, ML050550198, (May 1962)

[27] J. V. Cathcart, R. E. Pawel, R. A. McKee, R. E. Druschel, G. J. Yurek, J. J. Campbell, and S. H. Jury, "Zirconium Metal-Water Oxidation Kinetics IV. Reaction Rate Studies", ORNL/NUREG-17, ML052230079, (August 1977)

[28] F. Nagase, T. Otomo, H. Uetsuka, Oxidation Kinetics of Low-Sn Zircaloy-4 at the Temperature Range from 773 to 1573K, Journal of Nuclear Science and Technology 40 (2003) 213-219.

[29] J.H. Baek, K.B. Park, Y.H. Jeong, Oxidation kinetics of Zircaloy-4 and Zr-1Nb-1Sn-0.1Fe at temperatures of 700-1200°C, Journal of Nuclear Materials 335 (2004) 443-456.

[30] M.C. Billone, Y. Yan, T. Burtseva, R. Daum, "Cladding Embrittlement during Postulated Loss-of-Coolant Accidents", NUREG/CR-6967, ML082130389, (July 2008)

[31] L. Portier, T. Bredel, JC. Brachet, V. Maillot, JP. Mardon, A. Lesbros, "Influence of Long Service Exposures on the Thermal-Mechanical Behavior of Zy-4 and M5 Alloys in LOCA Conditions," Journal of ASTM International, Vol. 2, No. 2 (2005) Paper JAI12468

[32] S. Leistikow, G. Schanz, Oxidation Kinetics and Related Phenomena of Zircaloy-4 Fuel Cladding Exposed to High Temperature Steam and Hydrogen-Steam Mixtures under PWR Accident Conditions, Nuclear Engineering and Design 103 (1987) 65-84.

[33] S. Leistikow, G. Schanz, H.V. Berg, A.E. Aly, Comprehensive presentation of extended Zircaloy-4 steam oxidation results (600-1600°C), OECD-NEA-CSNI/IAEA Specialists Meeting on Water Reactor Fuel Safety and Fission Product Release in Off-Normal and Accident Conditions, Risö National Laboratory, Denmark, 1983.

[34] J.H. Baek, Y.H. Jeong, Breakaway phenomenon of Zr-based alloys during a high-temperature oxidation, Journal of Nuclear Materials 372 (2008) 152-159.

[35] J.A. Gresham, Updated Westinghouse Breakaway Oxidation Testing/Behavior (Non-Proprietary), Westinghouse letter report to NRC LTR-NRC-08-29, US NRC ADAMS Accession No. ML081700587, 2008.

[36] Z. Hózer, C. Gyori, L. Matus, M. Horváth,, Ductile-to-brittle transition of oxidised Zircaloy-4 and E110 claddings, Journal of Nuclear Materials 373 (2008) 415-423.

[37] D.J. Park, J.Y. Park, Y.H. Jeong, J.Y. Lee, Microstructural characterization of ZrO2 layers formed during the transition to breakaway oxidation, Journal of Nuclear Materials 399 (2010) 208-211.

[38] H.H. Kim, J.H. Kim, J.Y. Moon, H.S. Lee, J.J. Kim, Y.C. Chai, Y.C., High-temperature Oxidation Behavior of Zircaloy-4 and Zirlo in Steam Ambient, Journal of Materials Science & Technology 26 (2010) 827-832.

[39] M. Große, Comparison of the high temperature steam oxidation kinetics of advanced cladding materials, Nuclear Technology 170 (2010) 272-279.

[40] M. Steinbrück, J. Birchley, A.V. Boldyrev, A.V. Goryachev, M. Große, T.J. Haste, Z. Hózer, A.E. Kisselev, V.I. Nalivaev, V.P. Semishkin, L. Sepold, J. Stuckert, N. Vér, M.S. Veshchunov, High-temperature oxidation and quench behaviour of Zircaloy-4 and E110 cladding alloys, Progress in Nuclear Energy 52 (2010) 19-36.

[41] H.K. Yueh, R.J. Comstock, B. Dunn, M. Le Saux, Y.P. Lin, D. Lutz, D.J. Park, E. Perez-Fero, Y. Yan, Loss of Coolant Accident Testing Round Robin, TopFuel 2013, Charlotte, NC, September 15–19, 2013, American Nuclear Society, La Grange Park, IL, USA.

[42] G. Hache, H.M. Chung, “The History of the LOCA embrittlement criteria”, Topical Meeting on LOCA Fuel Safety Criteria held in Aix-en-Provence, OECD- NEA, (2001), pp. 37-64

[43] C. Grandjean, G. Hache, “A State-Of-the-Art Review of past programmes devoted to fuel behavior under LOos-of-Coolant-Accident conditions. Part 3: Cladding oxidation. Resistance to quench and post-quench loads”, IRSN Technical Report, DPAM/SEMCA 2008-093, (2008), p.28

[44] “State-of-the-art Report Nuclear on Fuel Behaviour in Loss-of-coolant Accident (LOCA) Conditions”, OECD Report, (2009), NEA No. 6846

[45] Atomic Energy Commission Rule-Making Hearing, Opinion of the Commission, Docket RM-50-1, (28 December, 1973)

[46] Atomic Energy Commission Rule-Making Hearing, Concluding Statement of the Regulatory, Staff, Docket RM-50-1, (16 April, 1973)

[47] Acceptance Criteria for Emergency Core Cooling Systems for Light-Water Nuclear Power Reactors, U.S. Code of Federal Regulations, Title 10, Part 50, Section 46 (1974)

[48] F. Nagase, T. Fuketa, “Behavior of Pre-hydrided Zircaloy-4 Cladding under Simulated LOCA Conditions”, Journal of Nucl. Sci. and Tech. 42 (2005) 209–218

[49] USNRC, “Technical basis for revision of embrittlement criteria in CFR 50.46”, Research information letter 0801, (May 30, 2008)

[50] USNRC, “Establishing Analytical Limits For Zirconium-Based Alloy Cladding”, RG 1.224, ML15238B155, (2016)

[51] S. Graff, S. Boutin, A. Foucher-Taisne, O. Dubois, “New LOCA and RIA fuel safety criteria in France”, Proceedings of WRFPM Conference, Jeju, Republic of South Korea, (September 2017)

[52] M.C. Billone, “Assessment of Current Test Methods for Post-LOCA Cladding Behavior”, NUREG/CR-7139, ML12226A182, August, 2012

[53] M.C. Billone, Y. Yan, T.A. Burtseva, R.O. Meyer, “Cladding Behavior during Postulated Loss-of-Coolant Accidents”, NUREG/CR-7219, ANL-16/09, (2016)

[54] USNRC, “Testing For Postquench Ductility”, RG 1.223, ML15238B079, (2016)

[55] D.O. Hobson P.L. and Rittenhouse, “Embrittlement of Zircaloy Clad Fuel Rods by Steam During LOCA Transients”, Oak Ridge National Laboratory, ORNL-4758, (January 1972)

[56] J.C. Brachet J. Pelchat, D. Hamon, R. Maury, P. Jacques, JP. Mardon, “Mechanical behavior at Room Temperature and Metallurgical study of Low-Tin Zy-4 and M5™ alloys after oxidation at 1100°C and quenching”, Proceedings of the Technical Committee Meeting on Fuel Behavior Under Transient and LOCA Conditions, IAEA-TECDOC-1320, Halden, Norway, (Sept 10–14, 2001), pp. 139-158

[57] J.C. Brachet, V. Maillot, L. Portier, D. Gilbon, A. Lesbros, N. Waeckel and J.P. Mardon, “Hydrogen Content, Pre Oxidation and Cooling Scenario Influences on Post-Quench Mechanical Properties of Zy-4 and M5™ Alloys in LOCA Conditions - Relationship with the Post-Quench Microstructure”, Journal of ASTM International, Vol. 5, No. 4 (2008) Paper JAI101116

[58] M. Le Saux, J.C. Brachet, V. Vandenberghe, D. Gilbon, J.P. Mardon, B. Sebbari, “Influence of Pre-Transient Oxide on LOCA High Temperature Steam Oxidation and Post-Quench Mechanical Properties of Zircaloy-4 and M5™ cladding”, 2011 Water Reactor Fuel Performance (Topfuel) Meeting, Chengdu, China, (Sept. 11-14, 2011), Paper T3-040

[59] J.C. Brachet, D. Hamon, J.L. Béchade, P. Forget, C. Toffolon-Masclet, C. Raepsaet, J.P. Mardon and B. Sebbari, “Quantification of the chemical elements partitioning within pre-hydrided Zircaloy-4 after high temperature steam oxidation as a function of the final cooling scenario (LOCA conditions) and consequences on the (local) materials hardening”, IAEA-TECDOC-CD-1709 (2013) 253-265

[60] J. Debuigne, “Contribution to Study of Zirconium Oxidation and oxygen Diffusion into the Oxide and the Metal”, PhD Thesis, Faculté des sciences de Paris – *in French* (1966)

[61] F. C. Iglesias, D. B. Duncan, S. Sagat, H. E. Sills, “Verification of the from model for zircaloy oxidation during high temperature transients”, Journal of Nuclear Materials 130 (1985) 36–44

[62] X. Ma, C. Toffolon-Masclet, T. Guilbert, D. Hamon, J.C. Brachet, “Oxidation kinetics and oxygen diffusion in low-tin Zircaloy-4 up to 1523 K”, Journal of Nuclear Materials 377 (2008) 359–369

[63] C. Corvalan-Moya, C. Desgranges, C. Toffolon-Masclet, C. Servant, J.C. Brachet, “Numerical modelling of oxygen diffusion in the wall thickness of low-tin zircaloy-4 fuel cladding tube during high temperature (1100°C-1250°C) steam oxidation”, Journal of Nuclear Materials 400 (2010) 196–204

[64] A. V. Berdyshev, M. S. Veshchunov, Proceedings of Nuclear Safety Institute (IBRAE-RAS), Vol. 1, pp. 6–14 (2010)

[65] C. Duriez, S. Guilbert, A. Stern, C. Grandjean, L. Belovsky, J. Desquines, “Characterisation of oxygen distribution in LOCA situations”, Journal of ASTM International, Vol. 2, No 8 (2010) Paper ID JAI103156

[66] H. Xiaoqiang, Y. Hongxing, J. Guangming. proceedings of 2011 Water Reactor fuel Performance Meeting Conference Proceeding T3-040, Chengdu, China, (Sept 11–14, 2011)

[67] B. Mazères, C. Desgranges, C. Toffolon-Masclet, D. Monceau, “Contribution to Modelling of Hydrogen Effect on Oxygen Diffusion in Zy-4 Alloy During High Temperature Steam Oxidation”, Oxid. Met. 79 (2013)121–133

[68] A. Sawatzki, G. A. Ledoux, S. Jones, “Oxidation of Zirconium During a High Temperature Transient”, Zirconium in the Nuclear Industry, ASTM STP 633, A. L. Lowe, Jr. and G. W. Parry, Eds., American Society for Testing materials, (1977), 134–149

[69] H.M. Chung and T.F. Kassner, “Embrittlement Criteria for Zircaloy Fuel Cladding Applicable to Accident Situations in Light-Water Reactors”, Summary Report, NUREG/CR-1344, ANL-7948, (1980)

[70] M. Négyesi, L. Novotný, J. Kabátová, S. Linhart, V. Klouček, J. Lorinčík, V. Vrtílková, “UJP LOCA Oxidation Criteria “K” and “Oβ””, IAEA-TECDOC-CD-1709, (2013)

[71] N. Dupin, I. Ansara, C. Servant, C. Toffolon, C. Lemaignan, JC. Brachet, “A Thermodynamic Database for Zirconium Alloys”, Journal of Nuclear Materials 275 (1999) 287-295

[72] P. Lafaye, “Développement d’outils de modélisation thermodynamiques pour la prédiction de l’état métallurgique d’alliages à base zirconium”, PhD Thesis, Paris-Est University (2017), in French

[73] N.B. Pilling, R.E. Bedworth, “The oxidation of metals at high temperatures”, J. Inst. Met. 29 (1923) 529–582

[74] P. Lafaye, C. Toffolon-Masclet, J.-C. Crivello, J.-M. Joubert « Experimental investigations and thermodynamic modelling of the Cr–Nb–Sn–Zr system”, Calphad 64, (2019), 43–54

[75] JC. Brachet, E. Rouesne, T. Guilbert, J. Ribis, M. Le Saux, G. Nony, H. Palancher, A. David, J. Bischoff, J. Augereau, E. Pouillier, “High Temperature Steam Oxidation of Chromium-Coated Zirconium-Based Alloys: Kinetics and Process”, Corrosion Science (2020), doi: https://doi.org/10.1016/j.corsci.2020.108537

[76] K.G. Geelhood and W.G. Luscher, “Degradation and Failure Phenomena of Accident Tolerant Fuel Concepts Chromium Coated Zirconium Alloy Cladding”, PNNL-28437 Report, Revision 1, (June 2019)

[77] “Applicability of Nuclear Fuel Safety Criteria to Accident Tolerant Fuel Designs, OECD-CSNI Technical Opinion Papers, to be published (2020)

FIGURE CAPTIONS:

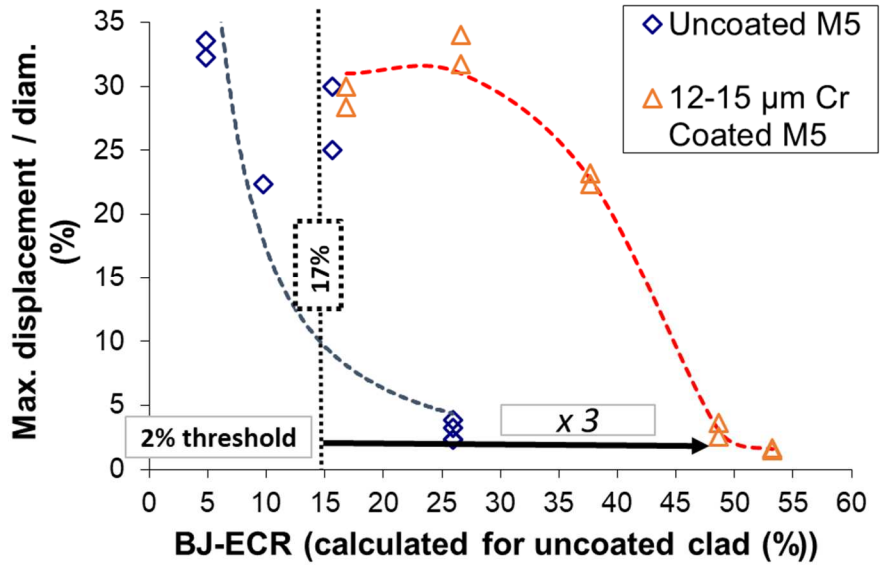

(a)

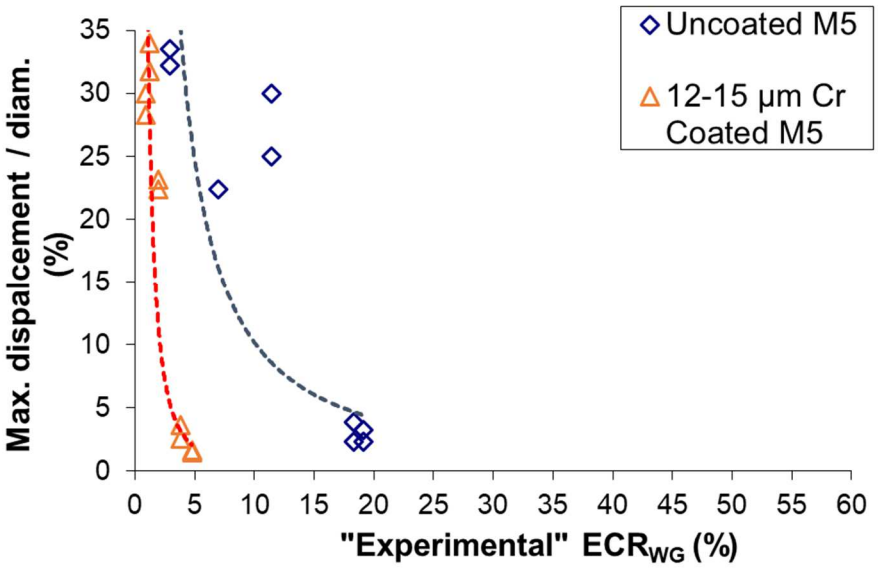

(b)

Figure 1 - PQ "residual ductility" of 12-15 µm Cr coated M5$_{Framatome}$ after one-sided steam oxidation at 1200 °C and direct water quench, deduced from RCT at 135 °C, in relation with BJ-ECR (a) and "experimental" (i.e., deduced from weight gain measurements) ECR (b);

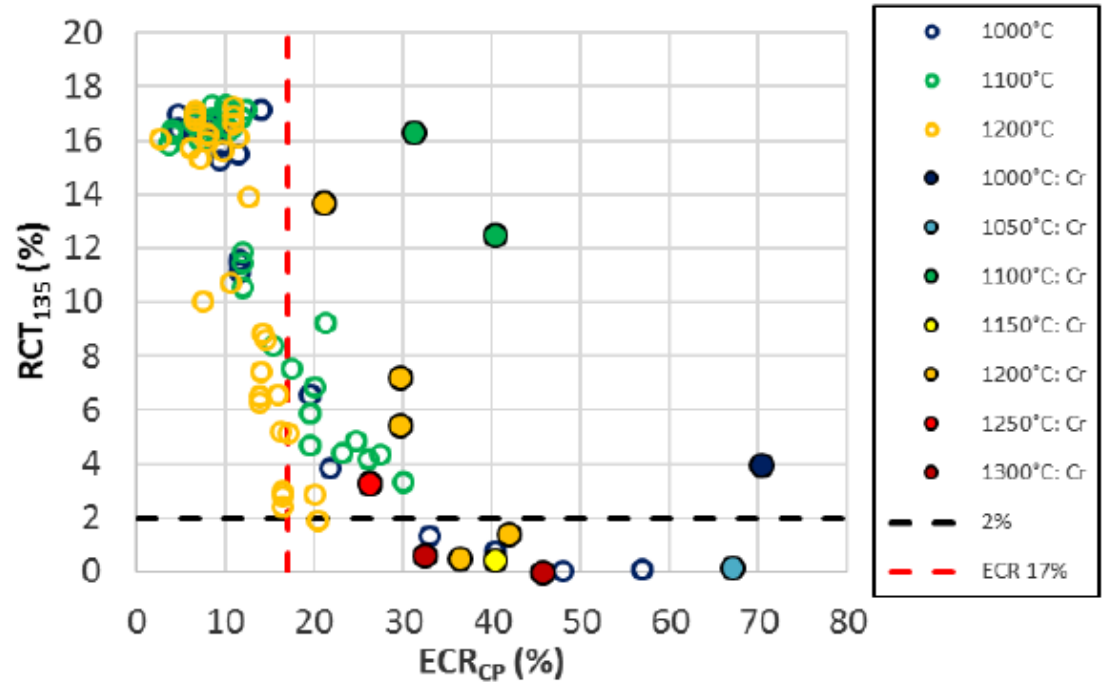

(a)

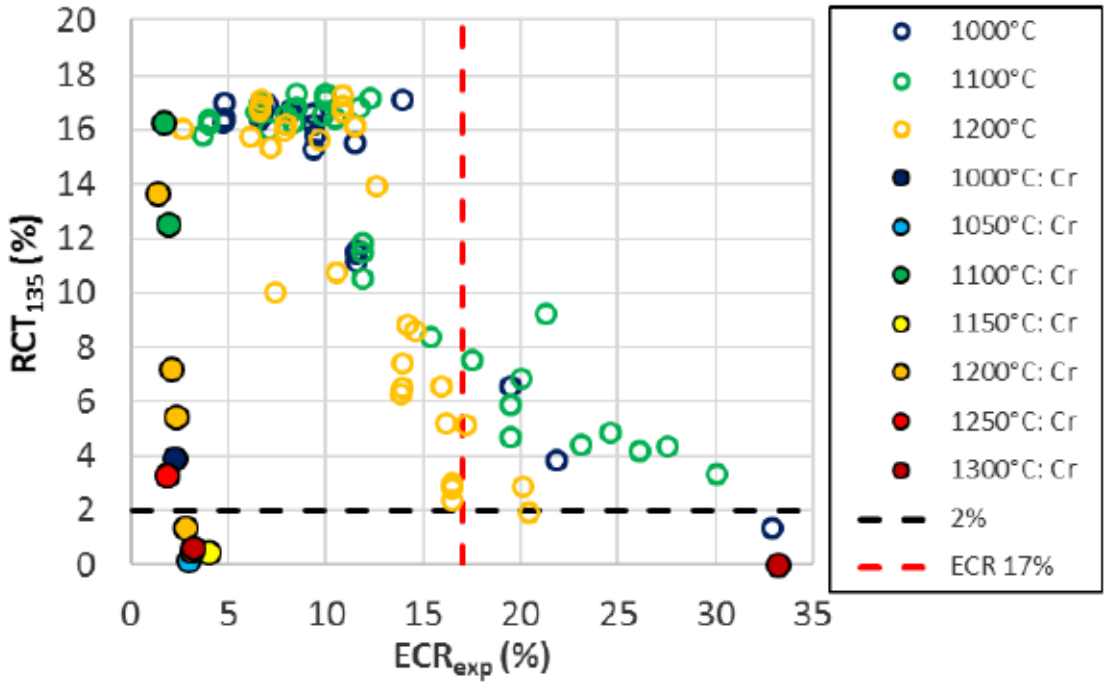

(b)

Figure 2 - (from [12]) – PQ "residual ductility" deduced from RCTs at 135 °C in relation with CP-ECR (a) and "experimental" (i.e., deduced from weight gain measurements) ECR (b); comparison of Cr-coated (full symbols) and uncoated (empty symbols) E110 (Zr1Nb) specimens.

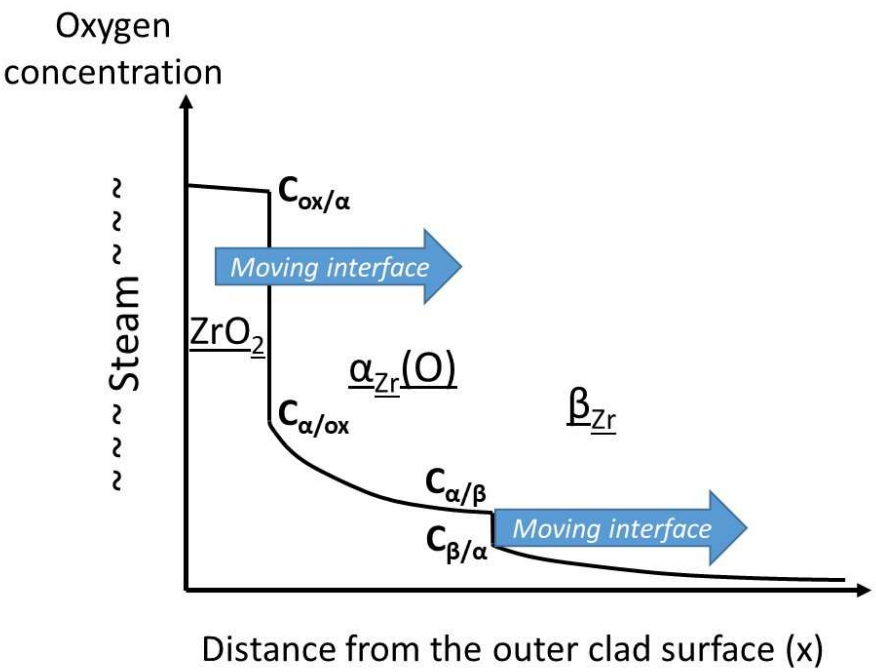

Figure 3 - Schematic diagram of phase thickness evolution and oxygen diffusion profile associated with the HT oxidation process of Zircaloy's type claddings, for oxidation temperature above the α+β/β transition temperature

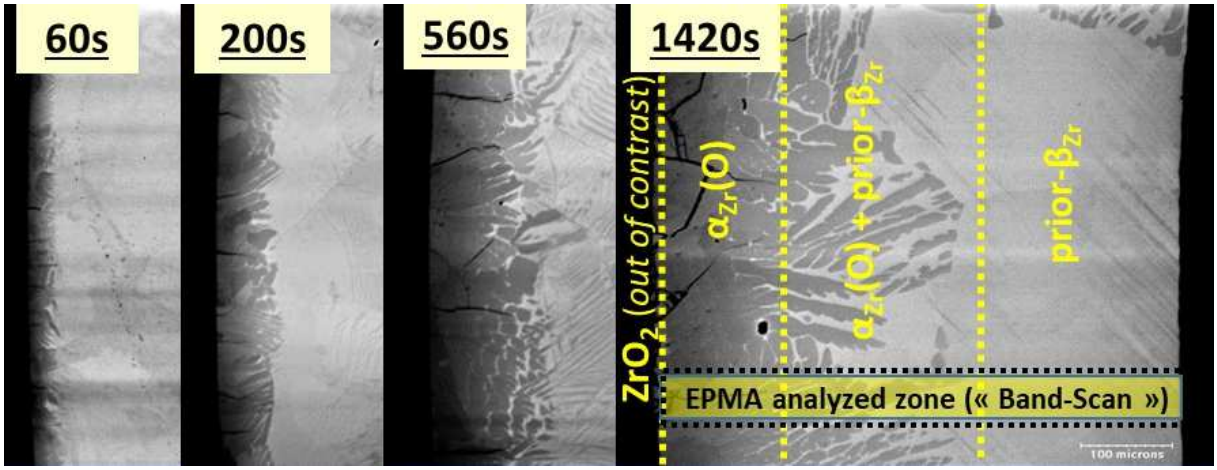

(a)

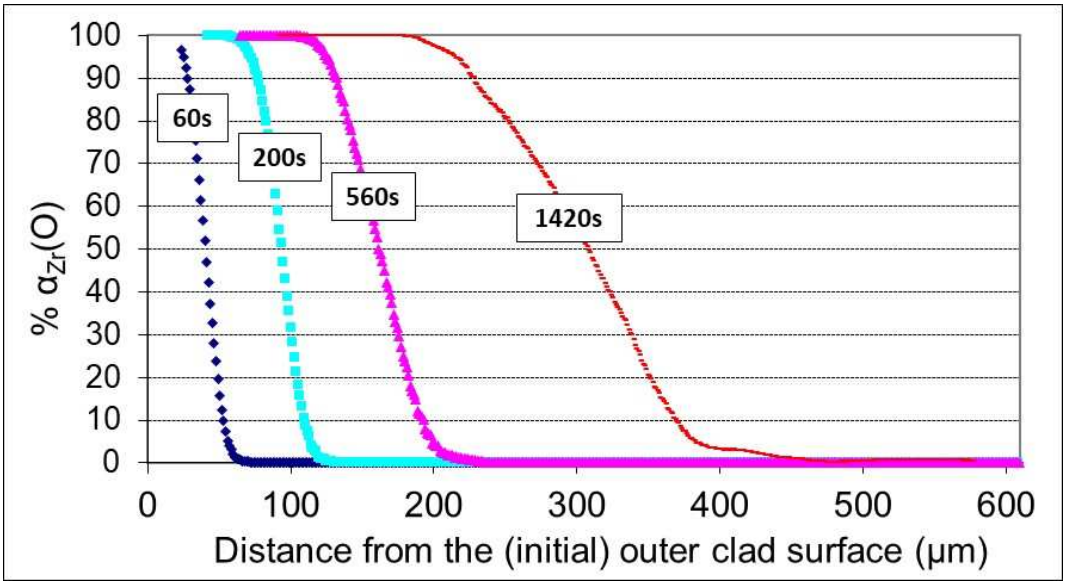

(b)

Figure 4 - SEM micrographs (BSE mode with amplified phase contrast) - (a) and corresponding $\alpha_{Zr}(O)$ fraction evolution measured by image analysis – (b) throughout the wall clad thickness of uncoated $M5_{Framatome}$, one-sided steam oxidized for different times at 1200 °C

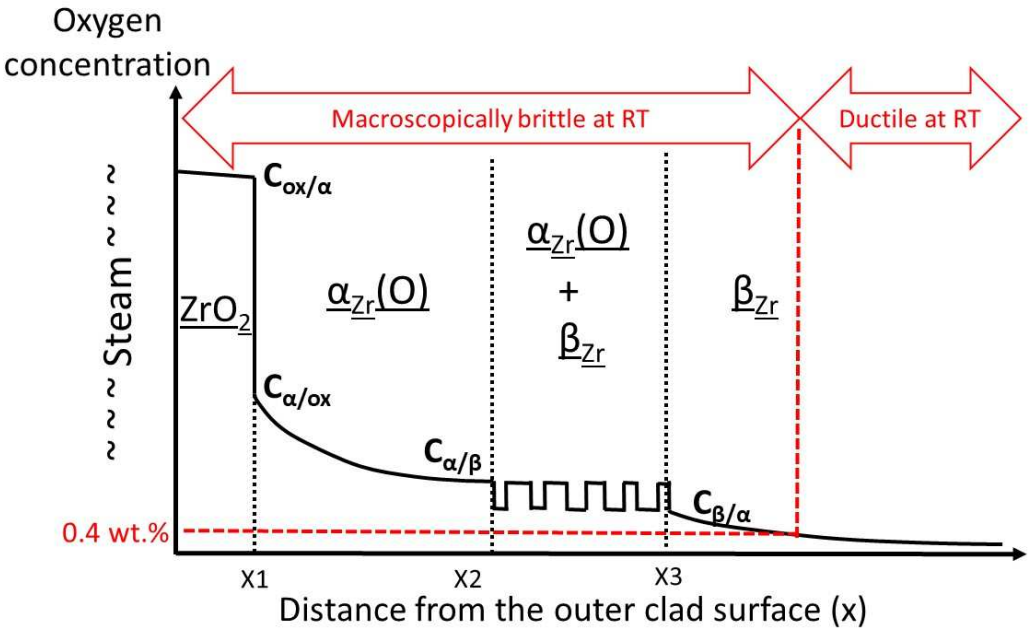

(a)

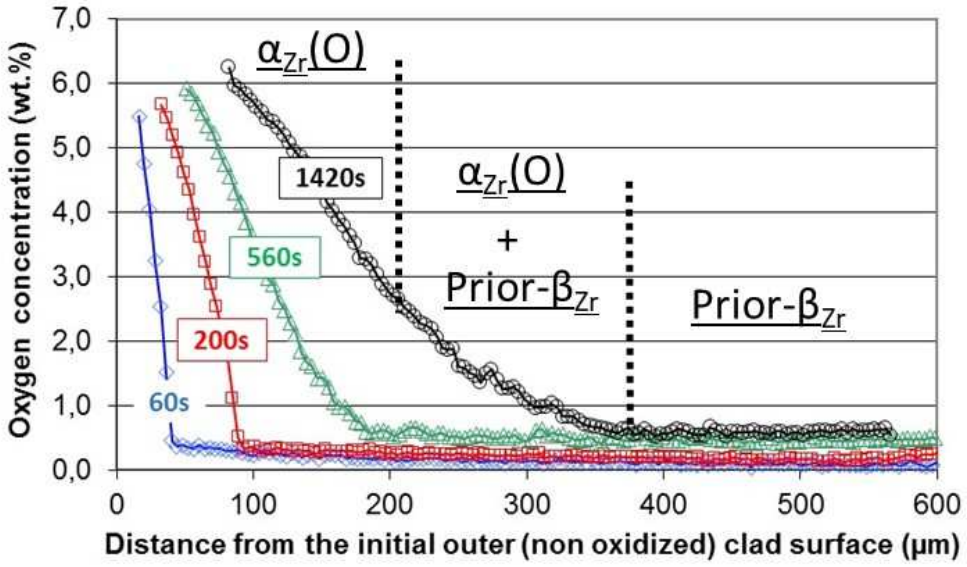

(b)

Figure 5 - Schematic (a) and EPMA ("50 µm-band-scan" mode) experimental oxygen diffusion profiles (b) measured after steam oxidation at 1200 °C of uncoated M5Framatome

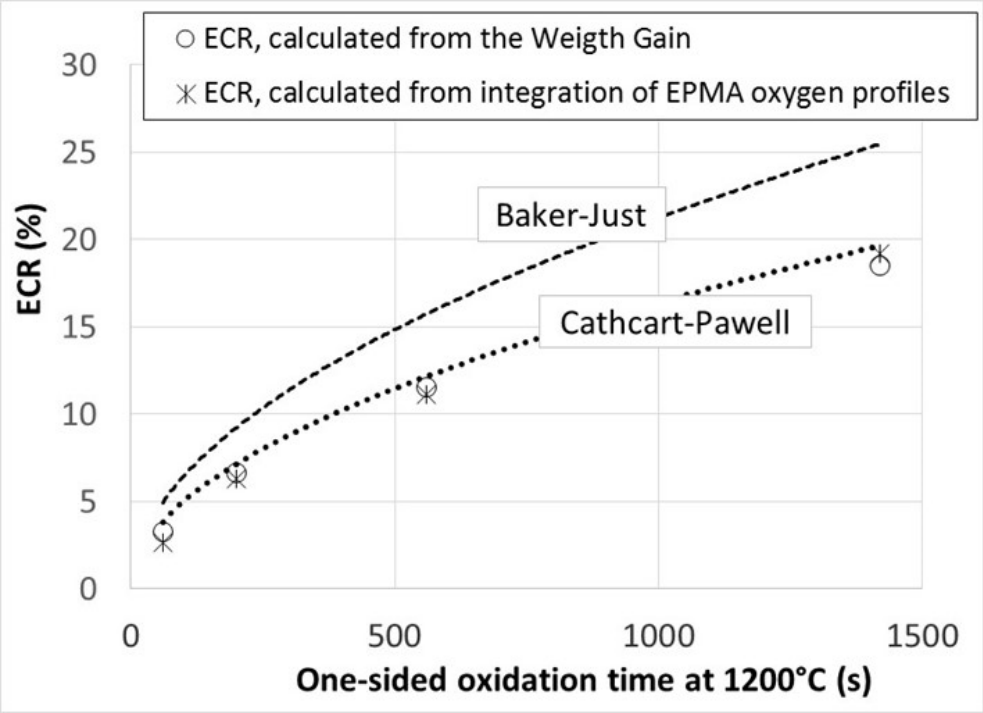

(b)

Figure 6 – Calculated vs. experimental ECR parameters evolutions as a function of one-sided steam oxidation time at 1200 °C of uncoated $M5_{Framatome}$

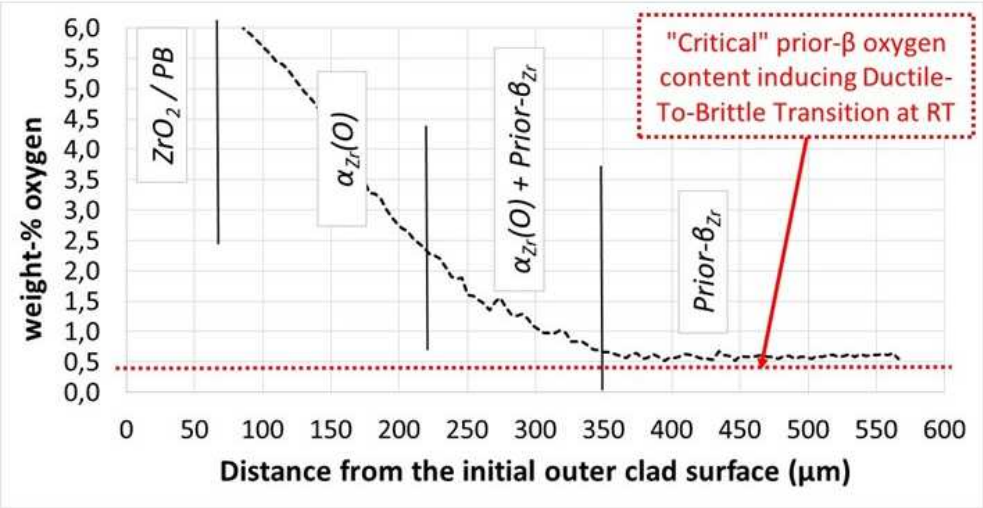

(a)

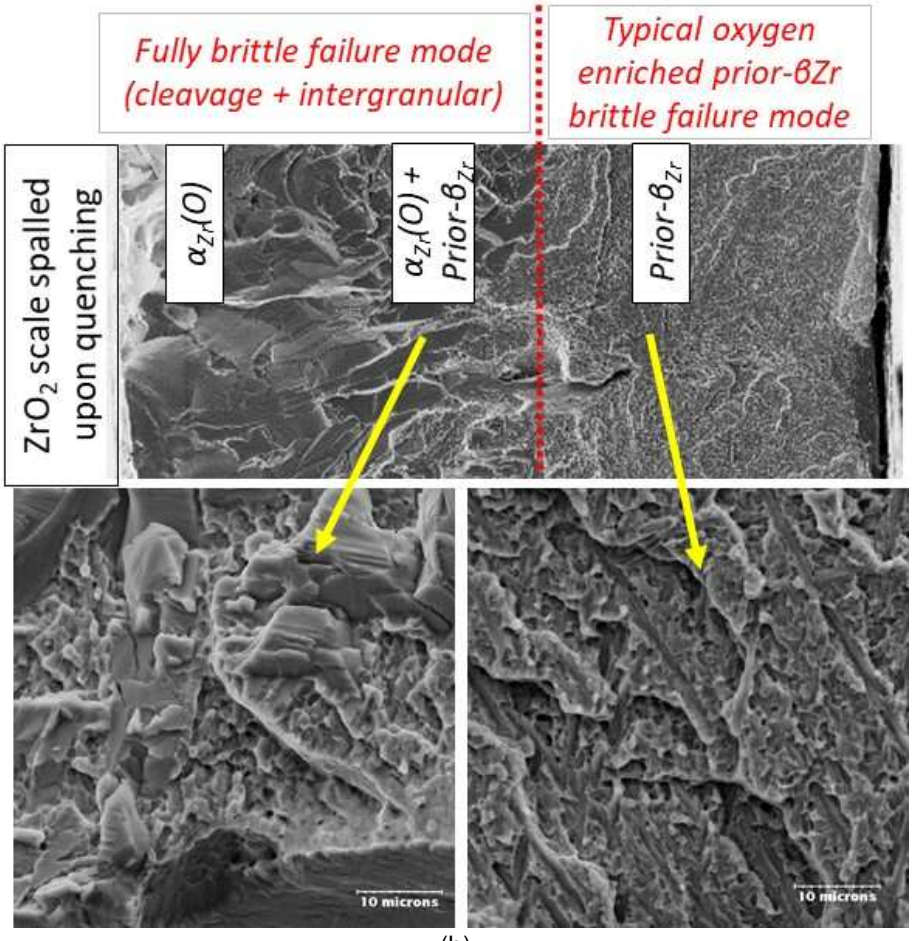

(b)

Figure 7 – Uncoated M5$_{Framatome}$ oxidized for 1500 s at 1200 °C and directly water quenched: EPMA oxygen profile and associated SEM micrograph (BSE Mode) – (a) Corresponding SEM fractographs after PQ RCT carried out at RT – (b)

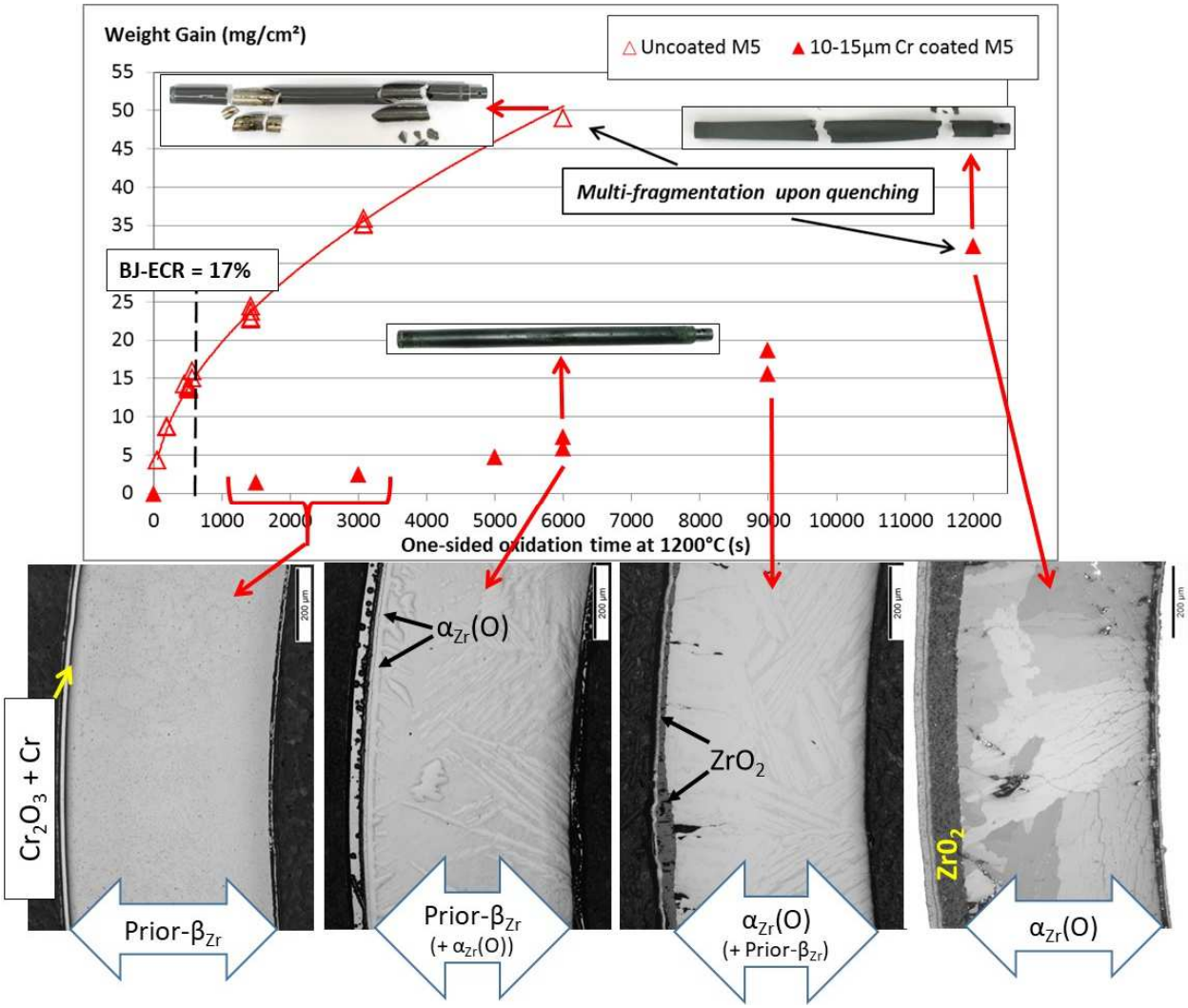

Figure 8 – Weight gain and associated photographs and optical micrographs of uncoated and 12-15 µm Cr-coated $M5_{Framatome}$ claddings as function of one-sided steam oxidation time at 1200 °C (followed by direct water quenching)

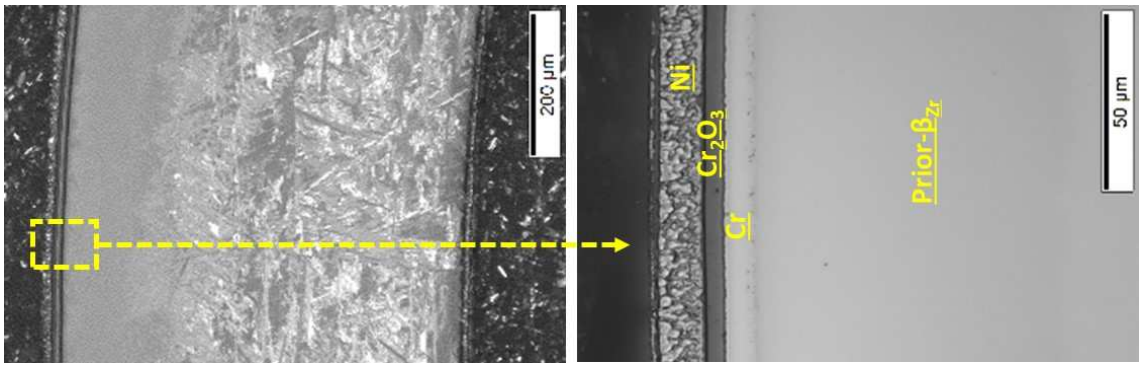

(a)

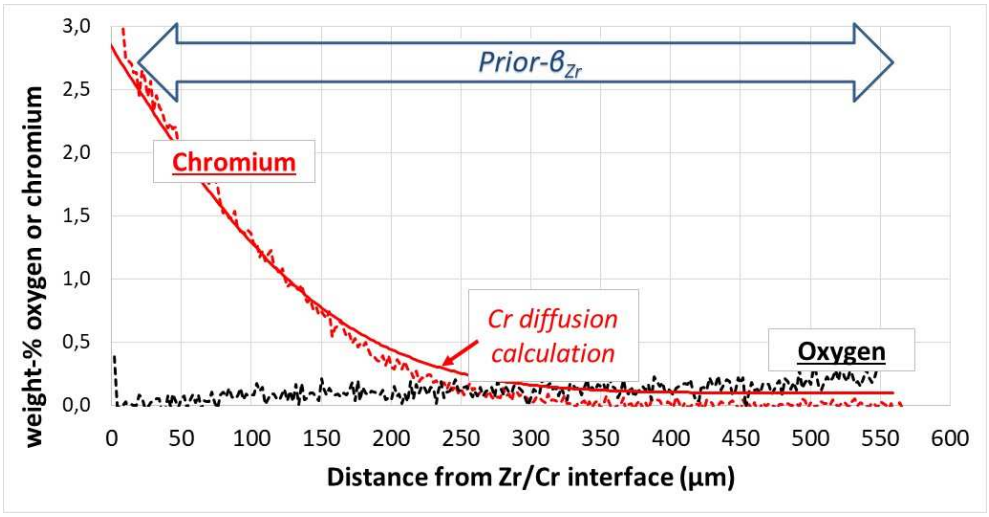

(b)

Figure 9 – Optical micrographs (a),
and diffusion profiles from EPMA (b)
of 12-15 µm Cr-coated $M5_{Framatome}$ one-sided steam oxidized for 1500 s at 1200 °C

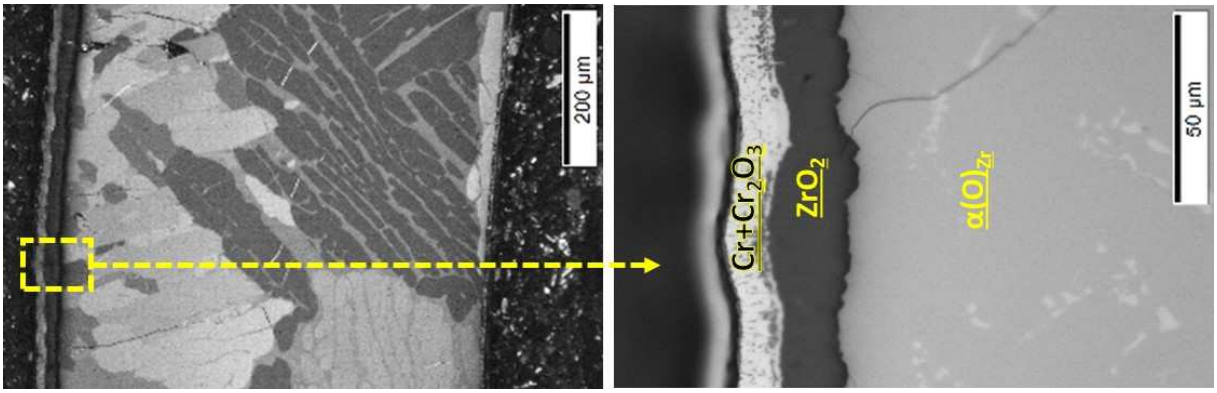

(a)

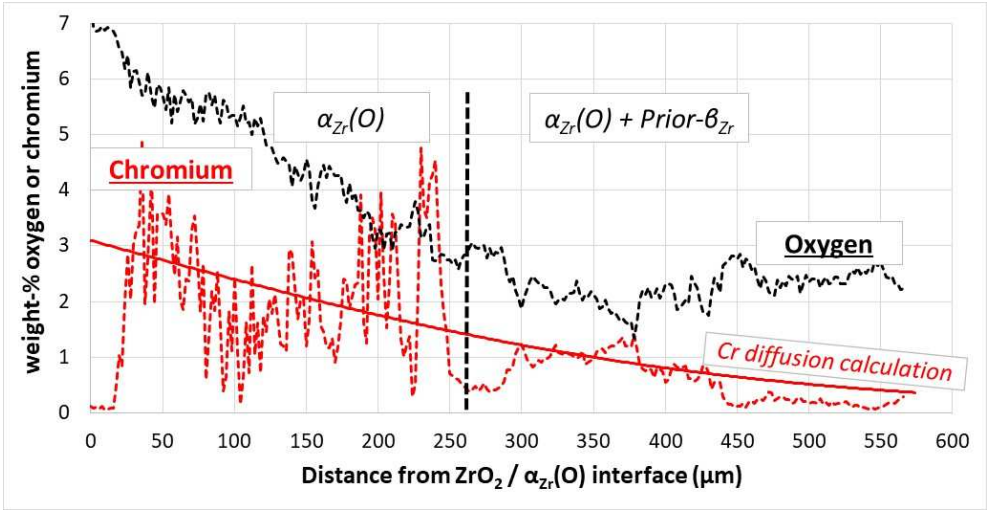

(b)

Figure 10 - Optical micrographs of 12-15 µm Cr-coated M5$_{Framatome}$ after one-sided steam oxidation for 9000 s at 1200 °C, followed by direct water quenching down to RT

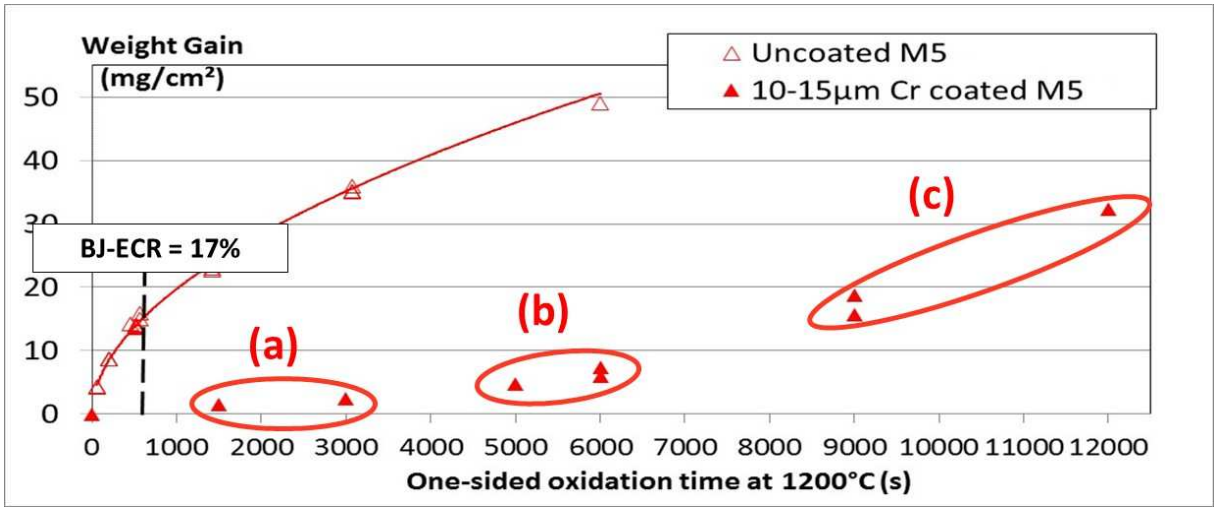

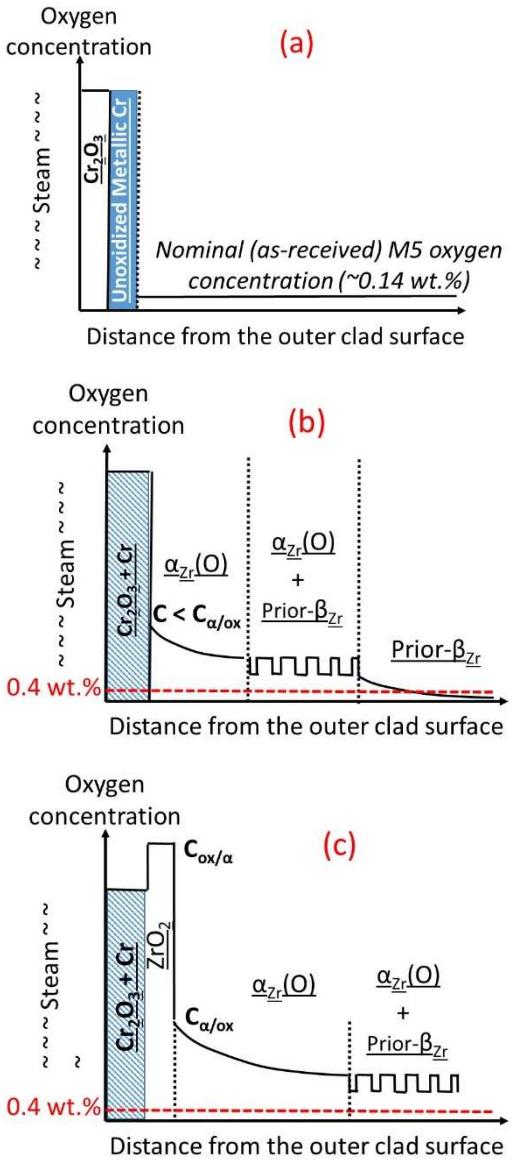

Figure 11 – Schematic representation of oxygen diffusion within the clad wall thickness of 12-15 µm Cr-coated M5Framatome upon one-sided steam oxidation at 1200 °C (see ref. [75] for more details on the underlying diffusion mechanisms)

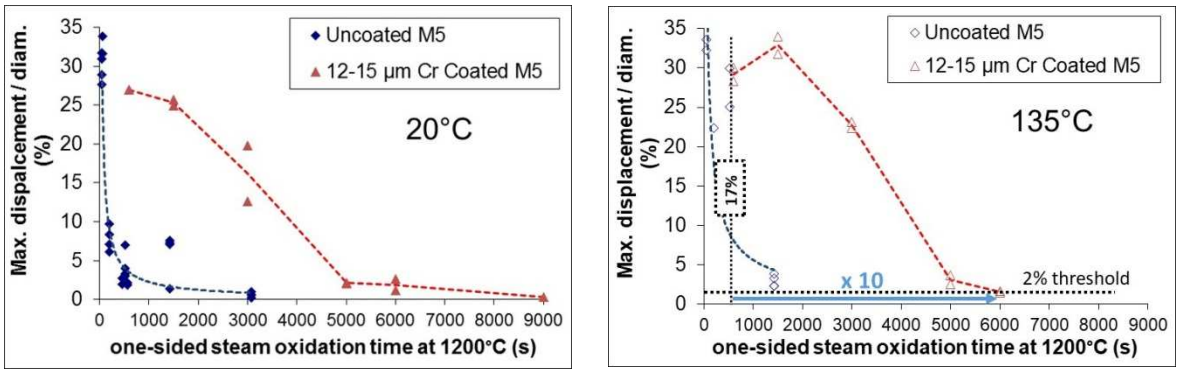

(a)

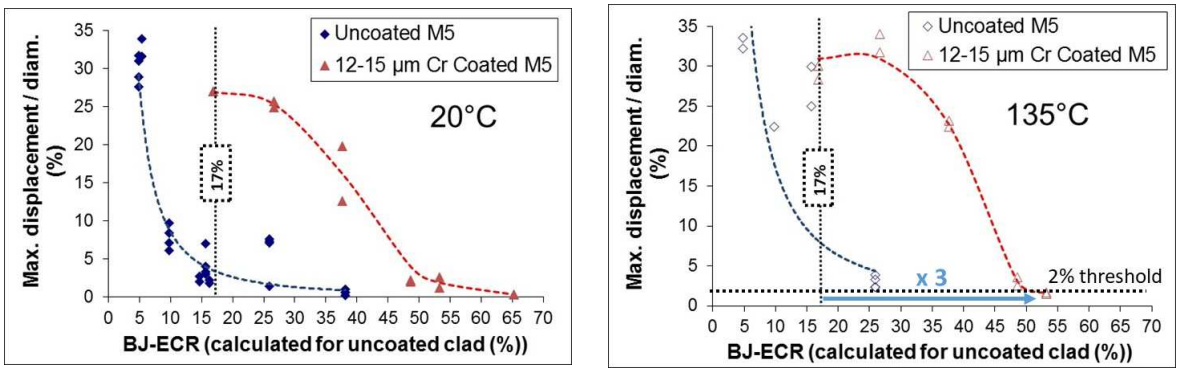

(b)

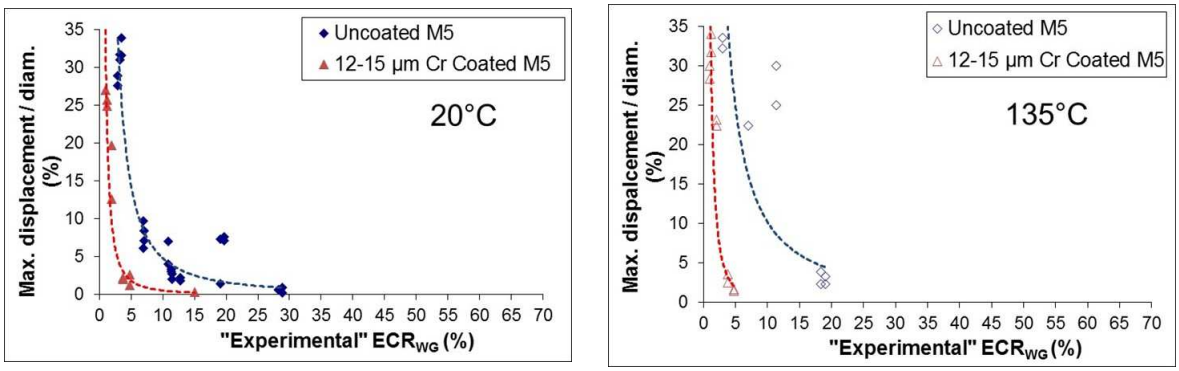

(c)

Figure 12 – Post-Quenching "residual ductility" derived from RCTs performed at 20 and 135 °C on uncoated and 12-15 µm Cr-coated M5$_{Framatome}$ as a function of: one-sided steam oxidation time at 1200 °C (a), ECR calculated using the BJ correlation (b) and ECR deduced from measured weight gain using the conventional correlations for the (uncoated) claddings (c)

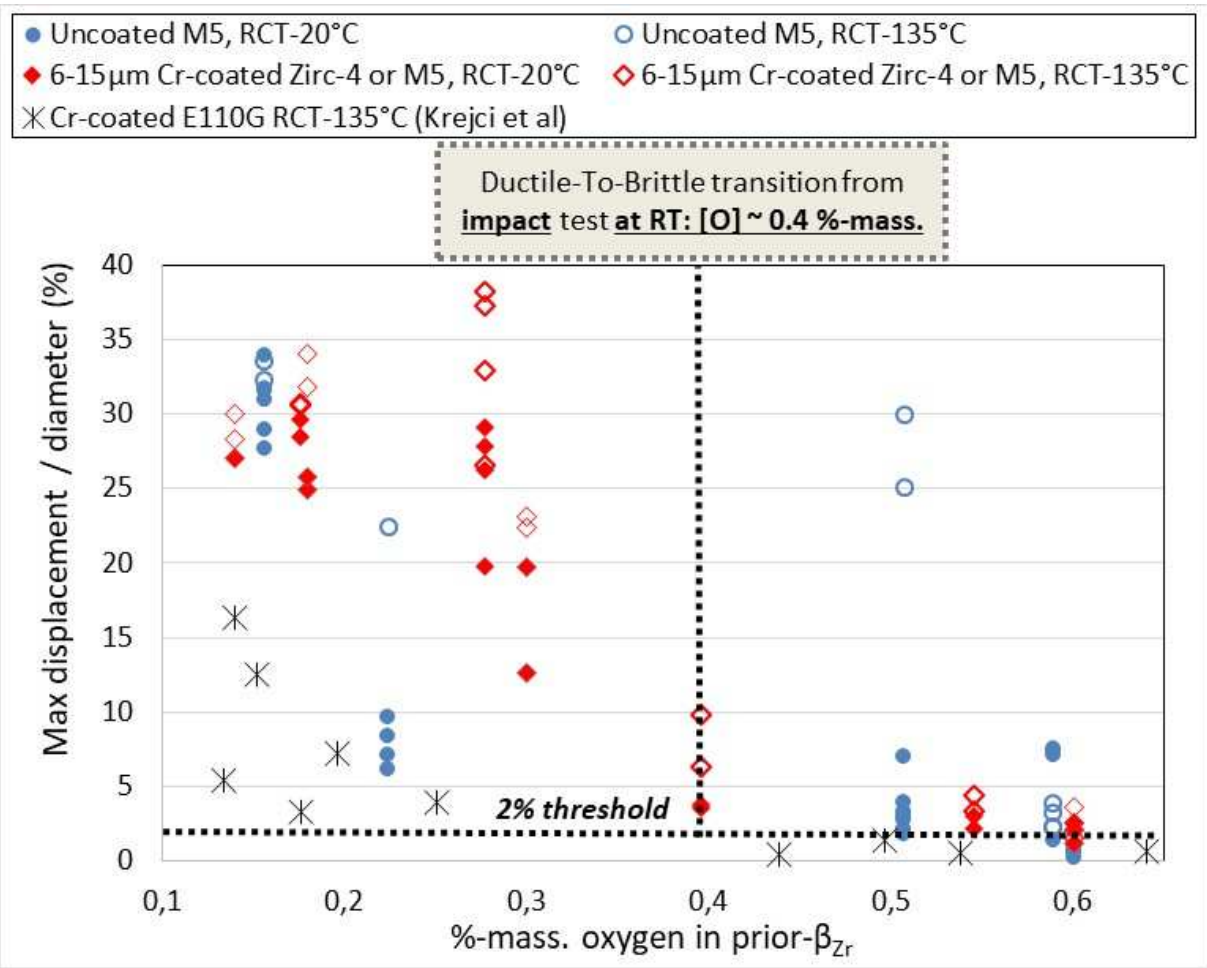

Figure 13 - Post-Quenching "residual ductility" derived from RCTs performed at 20 and 135 °C on uncoated and 6 to 15 µm thick Cr-coated zircaloy-4 or M5$_{Framatome}$, and from Krejci et al. on Cr-coated E110G substrate [12], as a function of the mean oxygen content of the residual prior-β$_{Zr}$ layer